HYDROLOGICAL PROCESSES
Hydrol. Process. **16**, 959–993 (2002)
Published online in Wiley InterScience (www.interscience.wiley.com). DOI: 10.1002/hyp.309

Geochemical weathering at the bed of Haut Glacier d'Arolla, Switzerland—a new model

M. Tranter,[1]* M. J. Sharp[2], H. R. Lamb[1], G. H. Brown[3], B. P. Hubbard[3] and I. C. Willis[4]

[1] *Bristol Glaciology Centre, School of Geographical Sciences, University of Bristol, Bristol BS8 1SS, UK*
[2] *Department of Earth and Atmospheric Sciences, University of Alberta, Edmonton, Alberta, Canada T6G 2E3*
[3] *Centre for Glaciology, Institute of Earth Studies, University of Wales, Aberystwyth SY23 3DB, UK*
[4] *Department of Geography, University of Cambridge, Cambridge CB3 3EN, UK*

Abstract:

Waters were sampled from 17 boreholes at Haut Glacier d'Arolla during the 1993 and 1994 ablation seasons. Three types of concentrated subglacial water were identified, based on the relative proportions of Ca^{2+}, HCO_3^- and SO_4^{2-} to Si. Type A waters are the most solute rich and have the lowest relative proportion of Si. They are believed to form in hydrologically inefficient areas of a distributed drainage system. Most solute is obtained from coupled sulphide oxidation and carbonate dissolution (SO–CD). It is possible that there is a subglacial source of O_2, perhaps from gas bubbles released during regelation, because the high SO_4^{2-} levels found (up to 1200 μeq/L) are greater than could be achieved if sulphides are oxidized by oxygen in saturated water at 0 °C (*c*. 414 μeq/L). A more likely alternative is that sulphide is oxidized by Fe^{3+} in anoxic environments. If this is the case, exchange reactions involving Fe^{III} and Fe^{II} from silicates are possible. These have the potential to generate relatively high concentrations of HCO_3^- with respect to SO_4^{2-}. Formation of secondary weathering products, such as clays, may explain the low Si concentrations of Type A waters. Type B waters were the most frequently sampled subglacial water. They are believed to be representative of waters flowing in more efficient parts of a distributed drainage system. Residence time and reaction kinetics help determine the solute composition of these waters. The initial water–rock reactions are carbonate and silicate hydrolysis, and there is exchange of divalent cations from solution for monovalent cations held on surface exchange sites. Hydrolysis is followed by SO–CD. The SO_4^{2-} concentrations usually are <414 μeq/L, although some range up to 580 μeq/L, which suggests that elements of the distributed drainage system may become anoxic. Type C waters were the most dilute, yet they were very turbid. Their chemical composition is characterized by low $SO_4^{2-}:HCO_3^-$ ratios and high pH. Type C waters were usually artefacts of the borehole chemical weathering environment. True Type C waters are believed to flow through sulphide-poor basal debris, particularly in the channel marginal zone. The composition of bulk runoff was most similar to diluted Type B waters at high discharge, and was similar to a mixture of Type B and C waters at lower discharge. These observations suggest that some supraglacial meltwaters input to the bed are stored temporarily in the channel marginal zone during rising discharge and are released during declining flow.

Little of the subglacial chemical weathering we infer is associated with the sequestration of atmospheric CO_2. The progression of reactions is from carbonate and silicate hydrolysis, through sulphide oxidation by first oxygen and then Fe^{III}, which drives further carbonate and silicate weathering. A crude estimate of the ratio of carbonate to silicate weathering following hydrolysis is 4 : 1. We speculate that microbial oxidation of organic carbon also may occur. Both sulphide oxidation and microbial oxidation of organic carbon are likely to drive the bed towards suboxic conditions. Hence, we believe that subglacial chemical weathering does not sequester significant quantities of atmospheric CO_2 and that one of the key controls on the rate and magnitude of solute acquisition is microbial activity, which catalyses the reduction of Fe^{III} and the oxidation of FeS_2. Copyright © 2002 John Wiley & Sons, Ltd.

INTRODUCTION

The hydrochemistry of glacier runoff has been used to infer hydrological flow paths (Collins, 1978, 1979; Sharp *et al*., 1995a) and the mechanisms of solute acquisition in subglacial environments (Raiswell, 1984;

* Correspondence to: Professor M. Tranter, Bristol Glaciology Centre, School of Geographical Sciences, University of Bristol, Bristol BS8 1SS, UK. E-mail: m.tranter@bristol.ac.uk

Received 13 March 2000
Accepted 21 January 2001

Souchez and Lemmens, 1987; Sharp, 1991; Tranter *et al*., 1993; Brown *et al*., 1994a). A fundamental problem with the interpretation of glacier hydrochemical time-series is that runoff issuing from the glacier terminus integrates the chemical composition of different water components, and information on the discharge and chemical composition of the components therefore is lost. Glacier hydrochemistry cannot easily be used to reconstruct the more complex aspects of subglacial drainage systems that have been revealed by recent borehole investigations (Fountain, 1994; Hubbard *et al*., 1995; Gordon *et al*., 1998) and the chemical reactions which might occur within them, without recourse to the direct measurement of the hydrochemistry of subglacial meltwaters (Tranter *et al*., 1997a).

Our current model of subglacial chemical weathering was inferred from runoff hydrochemistry at Haut Glacier d'Arolla (Tranter *et al*., 1993). It is successful apparently at describing the first-order chemical characteristics of bulk glacial runoff, which are believed to arise from the carbonation of rock flour with atmospheric CO_2 and the coupling of carbonate dissolution and sulphide oxidation. We believed that the model was readily transportable to other glaciated catchments because water–rock interactions were dominated by those involving carbonates and sulphides, which are trace components of many bedrocks (Holland, 1978). The model showed that glacier runoff chemistry is the consequence of the chemical evolution of waters flowing along relatively diffuse basal flowpaths and the dilution of these water within major basal drainage arteries, confounded by additional chemical evolution of the mixed waters en route to the glacier terminus.

The model falls short in explaining the following critical aspects of the chemistry of subglacial waters sampled from boreholes, suggesting that it is fundamentally flawed. First, SO_4^{2-} concentrations may exceed 1000 μeq/L (Lamb *et al*., 1995), requiring either that waters input to the subglacial drainage system are *c*. 250% saturated with respect to atmospheric O_2 or that there is a subglacial source of oxidizing agents, such as O_2. Second, waters flowing in the distributed component of the drainage system have an excess of HCO_3^- with respect to SO_4^{2-} (Tranter *et al*., 1997a). This suggests either that there is a subglacial source of CO_2 or that a key subglacial chemical weathering reaction has been missed. Third, the presence of microbial populations at the glacier bed (Sharp *et al*., 1999) suggests that oxidation of carbon, as well as sulphides, is possible, exacerbating the need for additional subglacial oxidizing agents to explain the elevated SO_4^{2-} concentrations. The existence of microbial communities in subglacial environments also suggests that chemical weathering in these environments may take place under suboxic conditions if oxidizing agents other than molecular oxygen can be utilized. Subglacial anoxia may explain why NO_3^- concentrations in bulk runoff decrease periodically to zero (Tranter *et al*., 1994). Finally, the existing model does not attempt to assess the relative proportions of the subglacial chemical weathering of carbonates and silicates, neither does it address whether or not kinetically rapid reactions such as carbonate and silicate hydrolysis or cation exchange impact on bulk meltwater chemistry. These four factors suggest that the current model of subglacial weathering at Haut Glacier d'Arolla is incomplete, and may not assess accurately the factors limiting the extent of subglacial chemical weathering. Here, we make fundamental revisions to this model after appraising critically the chemistry of samples collected from 17 boreholes drilled to the bed of Haut Glacier d'Arolla during two melt seasons (July through September, 1993 and 1994).

The following discussion of borehole water chemistry requires a knowledge of both our current understanding of subglacial chemical weathering and the nature of the subglacial drainage system at Haut Glacier d'Arolla. Both are summarized below, following the site description.

FIELD SITE

Haut Glacier d'Arolla is a warm-based glacier situated at the head of the Val d'Hérens, Valais, Switzerland (Figure 1). Approximately 54% of the 11·7 km^2 catchment area is glacierized. The glacier is *c*.4 km long and spans an elevation range of 2560–3500 m. Meltwater issues from several portals at the glacier snout, which exhibit marked differences in the colour and concentration of suspended sediment (Sharp *et al*., 1993). The glacier is underlain mainly by schistose granite (Figure 1a). Gneiss and greenschist outcrop in the vicinity

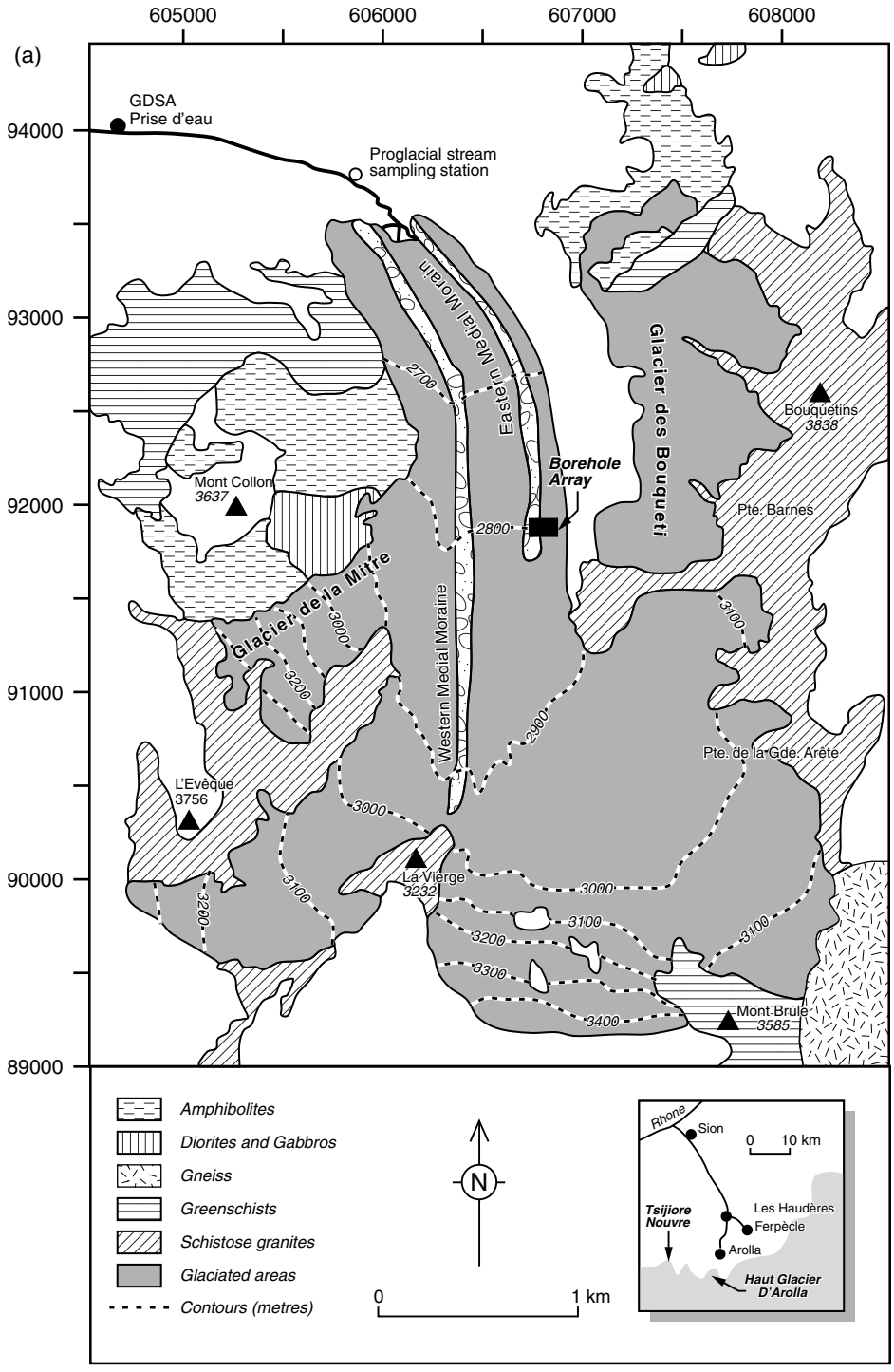

Figure 1. (a) Location map of Haut Glacier d'Arolla, also showing the bedrock geology

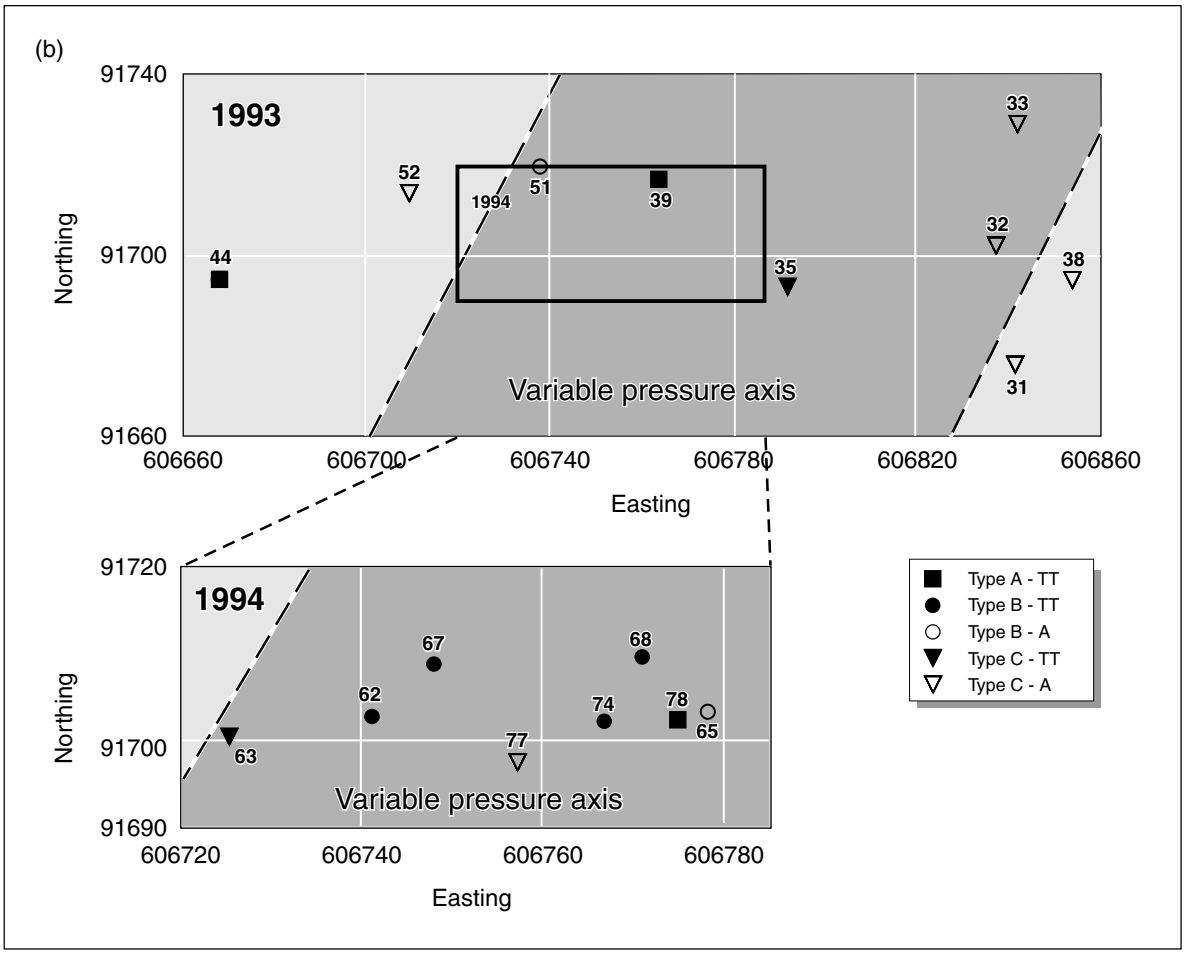

Figure 1. (b) Location of the variable pressure axis (VPA), as defined by Hubbard *et al*. (1995), in relation to the location of boreholes. Also shown are the different water types associated with the holes: TT denotes a true Type A, B or C water, whereas A denotes an artefact water composition

of Mont Brulé to the south-east. The lower part of the glacier to the north-west is underlain by amphibolite, greenschist and a gabbro intrusion (Mont Collon). The mineralogy of the bedrock comprises quartz, feldspars (including albite, anorthite and sanidine), pyroxenes (including diopside, enstatite and spodumene), mica, amphibole, cordierite, haematite, magnetite and talc. Carbonates and sulphides are present in trace quantities (0·00–0·58% and <0·005–0·71% respectively; S. H. Bottrell, personal communication; Tranter *et al*., 1997b). There are occasional carbonate veins in the schistose granite.

Current understanding of the subglacial drainage system

The subglacial drainage system is thought to consist of two main components, a distributed or 'slow' system (Fountain and Walder, 1998) and a discrete channelized, conduit or 'fast' system. The slow system transports a significant proportion of snowmelt (Richards *et al*., 1996), and may consist of a spectrum of elements, such as water-filled linked cavities (Kamb, 1986), films derived from basal melting (Weertman, 1972), broad, low canals (Walder and Fowler, 1994) and water-saturated till (Fountain, 1992), each of which may have very different chemical characteristics. The slow system feeds into the channelized, fast system, which is believed

to be a series of arterial channels or tunnels at the glacier bed. The fast system is fed directly by icemelt routed to the bed via moulins and crevasses, and by snowmelt routed through the slow system. The configuration of the subglacial drainage system is not static throughout the ablation season because the channelized system expands headwards at the expense of the distributed system, at a rate largely controlled by the retreat of the snowline (Nienow *et al*., 1998).

Hubbard *et al*. (1995) suggested that the major arterial channels at the bed in the vicinity of the borehole array (Figure 1) are flanked by an extensive channel marginal zone, located within or above a vertically confined sediment layer. Water is forced out of the channel and into this zone as a result of the high water pressures that build up during diurnal periods of increasing discharge. Water returns to the channel during periods of falling discharge. Fine sediment may be eluted from the channel marginal zone during the diurnal ebb and flow of channel-derived waters. The distribution of till at the bed is likely to be patchy (Harbor *et al*., 1997; Gordon *et al*., 1998), and it follows that the hydrological properties of the channel marginal zone are likely to be spatially variable also.

Current understanding of subglacial chemical weathering at Haut Glacier d'Arolla:

Two types of chemical weathering reactions are believed to occur in subglacial environments, namely carbonation reactions and the coupled reactions of sulphide oxidation and carbonate dissolution (Tranter *et al*., 1993). Carbonation of silicates and carbonates is described by Equations (1) and (2) (Table I) respectively, and is thought to occur mainly in major subglacial arterial channels using atmospheric CO_2 as a proton source. However, a number of other subglacial CO_2 sources may exist. These include pockets of air trapped in subglacial cavities, gas bubbles in glacier ice (Coachman *et al*., 1958) and microbial oxidation of organic carbon (Equation 3). Subglacial organic carbon may originate from freshly comminuted rock, material washed from the glacier surface or overridden soils and vegetation. These additional sources of CO_2 suggest that carbonation is not necessarily confined to major subglacial channels. The rate of carbonation is controlled by the rate at which CO_2 enters solution and the rate of dissolution of rock flour.

The dominant chemical weathering reactions in the slow drainage system are believed to be carbonate dissolution and sulphide oxidation, as described by Equation (4). The rate of sulphide oxidation is controlled by the dissolved oxygen content and pH of the waters, as well as by factors such as temperature, surface area and the concentrations of Fe^{2+} and Fe^{3+} (Nicholson *et al*., 1988; Moses and Herman, 1991; Williamson and Rimstidt, 1994). The dissolution of carbonate that accompanies sulphide oxidation maintains a relatively high pH, so promoting high rates of sulphide oxidation despite the decline in dissolved oxygen concentrations as the reaction proceeds. Ultimately, microbial activity is likely to be the dominant influence on the rate of sulphide oxidation in subglacial environments. Simple laboratory experiments demonstrate that microbially catalysed rates of oxidation can be at least two orders of magnitude greater than inorganic rates (Sharp *et al*., 1999).

The amount of SO_4^{2-} produced by Equation (4) is dependent on factors such as the availability of dissolved O_2 and reactive sulphides. The solubility of O_2 in water at 0 °C at the altitude of the glacier terminus is *c*. 11 mL/L (*c*. 362 μmol/L), although most supraglacial waters appear to be undersaturated (*c*. 30–90%; Brown *et al*., 1994b) with respect to atmospheric O_2. The stoichiometry of Equation (4) suggests that *c*. 386 μeq/l of SO_4^{2-} will be produced from O_2 saturated water at this altitude (if there are no other inputs of O_2 or oxidizing agents). Reactive sulphides, here defined as comminuted sulphides with surface dislocations, amorphous zones or microparticles (Petrovic, 1981), are believed to be largely exhausted in the distributed drainage system (Tranter and Raiswell, 1991), so that relatively little sulphide oxidation occurs in the channelized drainage system. This is because relatively low concentrations of SO_4^{2-} are found in waters at maximum diurnal and seasonal discharge, despite the generally higher concentrations of suspended sediment that are found at these times (Gurnell, 1987). Further, dissolution experiments using previously wetted proglacial sediment liberate relatively low concentrations of SO_4^{2-} with respect to Ca^{2+} and HCO_3^- over the first 3 hr of rock–water contact (Brown *et al*., 1994a).

Table I. Equations describing the principal geochemical weathering reactions in subglacial environments

Equation 1. Carbonation of feldspar surfaces

$$\underset{\text{anorthite (Ca-feldspar)}}{CaAl_2Si_2O_8(s)} + 2CO_2(aq) + 2H_2O(l) \rightleftharpoons Ca^{2+}(aq) + 2HCO_3^-(aq) + \underset{\text{weathered feldspar surfaces}}{H_2Al_2Si_2O_8(s)}$$

Equation 2. Carbonation of carbonate

$$\underset{\text{(Mg-)calcite}}{Ca_{1-x}(Mg_x)CO_3(s)} + CO_2(aq) + H_2O(l) \rightleftharpoons (1-x)Ca^{2+}(aq) + xMg^{2+}(aq) + 2HCO_3^-(aq)$$

Equation 3. Oxidation of organic carbon

$$C_{org}(s) + O_2(aq) + H_2O(l) \rightleftharpoons CO_2(aq) + H_2O(l) \rightleftharpoons H^+(aq) + HCO_3^-(aq)$$

Equation 4. Sulphide oxidation coupled to carbonate dissolution

$$\underset{\text{pyrite}}{4FeS_2(s)} + 16Ca_{1-x}(Mg_x)CO_3(s) + 15O_2(aq) + 14H_2O(l) \rightleftharpoons 16(1-x)Ca^{2+}(aq) + 16xMg^{2+}(aq) + 16HCO_3^-(aq) + 8SO_4^{2-}(aq) + \underset{\text{ferric oxyhydroxides}}{4Fe(OH)_3(s)}$$

Equation 5. Sulphide oxidation coupled to feldspar dissolution

$$4FeS_2(s) + \underset{\text{alkali feldspar}}{16Na_{1-x}K_xAlSi_3O_8(s)(s)} + 15O_2(aq) + 86H_2O(l) \rightleftharpoons 16(1-x)Na^+(aq) + 16xK^+(aq) + 8SO_4^{2-}(aq) + \underset{\text{kaolinite}}{4Al_4Si_4O_{10}(OH)_8(s)} + 32H_4SiO_4(aq) + 4Fe(OH)_3(s)$$

Equation 6. Carbonate hydrolysis

$$Ca_{1-x}(Mg_x)CO_3(s) + H_2O(l) \rightleftharpoons (1-x)Ca^{2+}(aq) + xMg^{2+}(aq) + HCO_3^-(aq) + OH^-(aq)$$

Equation 7. Feldspar hydrolysis

$$KAlSi_3O_8(s) + H_2O(l) \rightleftharpoons \underset{\text{weathered feldspar surfaces}}{HAlSi_3O_8} + K^+(aq) + OH^-(aq)$$

Equation 8. Silica hydrolysis

$$\underset{\text{silica}}{SiO_2(s)} + 2H_2O(l) \rightleftharpoons \underset{\text{silicic acid}}{H_4SiO_4(aq)}$$

Equation 9. Pyroxene hydrolysis

$$\underset{\text{forsterite}}{Mg_2Si_2O_6(s)} + 6H_2O(l) \rightleftharpoons 2Mg^{2+}(aq) + 4OH^-(aq) + 2H_4SiO_4(aq)$$

Equation 10. Formation of kaolinite from K-feldspar

$$\underset{\text{K-feldspar}}{4KAlSi_3O_8(s)} + 22H_2O(l) \rightleftharpoons 4K^+(aq) + 4OH^-(aq) + Al_4Si_4O_{10}(OH)_8(s) + 8H_4SiO_4(aq)$$

Table I. (*Continued*)

Equation 11. Dissolution of gypsum

$$\underset{\text{gypsum}}{CaSO_4 \cdot 2H_2O(s)} \rightleftharpoons Ca^{2+}(aq) + SO_4{}^{2-}(aq) + 2H_2O(l)$$

Equations 12–14. Oxidation of sulphide by oxygen

$$FeS_2(s) + 14Fe^{3+}(aq) + 8H_2O(l) \rightleftharpoons 15Fe^{2+}(aq) + 2SO_4{}^{2-}(aq) + 16H^+(aq) \quad (12)$$

$$14Fe^{2+}(aq) + 7/2\ O_2(aq) + 14H^+(aq) \rightleftharpoons 14Fe^{3+}(aq) + 7H_2O(l) \quad (13)$$

$$FeS_2(s) + 7/2\ O_2(aq) + H_2O(l) \rightleftharpoons Fe^{2+}(aq) + 2SO_4{}^{2-}(aq) + 2H^+(aq) \quad (14)$$

Equation 15. Oxidation of sulphide by ferric ions

$$FeS_2(s) + 14Fe^{3+}(aq) + 8H_2O(l) + 16CaCO_3(s) \rightleftharpoons 15Fe^{2+}(aq) + 16Ca^{2+}(aq) + 2SO_4{}^{2-}(aq) + 16HCO_3{}^-(aq)$$

Equations 16a and 16b. Examples of the oxidation of sulphide by Fe^{III} that, when coupled to carbonate dissolution, give $SO_4{}^{2-}$: $HCO_3{}^-$ ratios of 1 : 1 (in equivalents)

$$FeS_2(s) + 14Fe(OH)_3(s) + 4CaCO_3(s) \rightleftharpoons 15Fe(OH)_2(s) + 4Ca^{2+}(aq) + 2SO_4{}^{2-}(aq) + 4HCO_3{}^-(aq) + 4H_2O(l) \quad (16a)$$

$$FeS_2(s) + 14Fe^{III} - silicate(s) + 38H_2O(l) + 4CaCO_3(s) \rightleftharpoons 15Fe(OH)_2(s) + 14H_3 - silicate + 4Ca^{2+}(aq) + 2SO_4{}^{2-}(aq) + 4HCO_3{}^-(aq) \quad (16b)$$

Equation 17. Hypothetical example of the oxidation of sulphide by Fe^{III} that, when coupled to carbonate dissolution, gives $SO_4{}^{2-}$: $HCO_3{}^-$ ratios of 1 : 4 (in equivalents)

$$FeS_2(s) + Fe^{III}_{14} - silicate(s) + 8H_2O(l) + 16CaCO_3(s) \rightleftharpoons Fe^{II}_{15}Ca_6 - silicate(s) + 10Ca^{2+}(aq) + 2SO_4{}^{2-}(aq) + 16HCO_3{}^-(aq)$$

Sulphide oxidation can be coupled to silicate weathering, as illustrated by Equation (5). However, the amount of coupled sulphide oxidation and silicate weathering is thought to be small, although unquantified, despite silicates being the dominant mineral group in glacial debris. This is because silicate dissolution kinetics are slow with respect to carbonates (Tranter *et al.*, 1993).

METHODS

Borehole water sampling

Boreholes were drilled during July and August in both 1993 and 1994, close to the eastern margin of the glacier (Figure 1b). The location of the drill site was chosen on the basis of theoretical reconstructions of the subglacial drainage system and dye tracing studies (Sharp *et al.*, 1993; Richards *et al.*, 1996), which predicted a major drainage channel beneath this part of the glacier during the melt season. Boreholes were drilled using the method described in Tranter *et al.* (1997a). The depths of the boreholes (Table II) generally were consistent with predictions of ice thickness derived from radar depth sounding (Sharp *et al.*, 1993), so it is believed that all holes reached the bed.

Water samples were collected from 17 boreholes using samplers modified from the design of Blake and Clarke (1991). They were constructed of acrylic plexiglass, 316 stainless steel and PTFE to minimize chemical contamination. Samples were collected from Holes 31, 32, 33, 35, 38, 39, 44, 51 and 52 in 1993, from Julian

Table II. Summary of borehole arrays drilled during 1993 and 1994 field seasons

Year	Dimensions of array (m)	Area of array (m^2)	Number of boreholes	Range of depths (m)
1993	464 × 66	3062	29	23–142
1994	103 × 13	1326	21	32–133

Day (hereafter JD) 200 to 235, and from Holes 62, 63, 65, 67, 68, 74, 77 and 78 in 1994, from JD 203 to 242. The number of samples collected was dependent on weather conditions and whether or not it was physically possible to lower the sampler down the hole. Waters discussed in this paper were sampled at or near the base of the holes (except for Holes 39, 44 and 78), or near to englacial inlets of concentrated waters (Holes 39, 44 and 78), which are discussed further below.

Bulk runoff sampling

Bulk runoff was sampled in order to set limits on the integrated chemical composition of waters output from the subglacial drainage system, at times approximating to maximum and minimum discharge (1000 and 1700 hours respectively) from JD 195 to 256 in 1993 and JD 198 to 247 in 1994. A site about 100 m from the glacier snout was chosen to allow sufficient mixing of output from the portals. Full details of sampling and treatment can be found in Gurnell *et al*. (1994).

Supraglacial water sampling

Supraglacial samples were collected in order to characterize ice-melt inputs to the subglacial drainage system. Samples were collected periodically between JD 199 and 259 (1993) and between JD 207 and 240 (1994) from a major supraglacial channel draining the eastern part of the glacier, near to the borehole array.

Snow sampling

A crude indication of the composition of snowmelt can be obtained from fresh snow samples that were collected on an event basis from a snowboard in the village of La Monta, some 4 km to the north-east of the glacier at an elevation of 1892 m, from JD 342 (1993) to 74 (1994) and JD 260 (1994) to 31 (1995).

Field measurement of pH and alkalinity

The pH and alkalinity were determined in the field on filtered samples using the method described in Tranter *et al*. (1997a). The precision of pH measurements was typically ±0·02 pH units. The precision of alkalinity determinations was *c*. ±5% for concentrations >100 μeq/L.

Laboratory analysis

Major cations (Ca^{2+}, Mg^{2+}, Na^{+} and K^{+}), anions (Cl^{-}, NO_3^{-}, SO_4^{2-}) and Si were determined using the method described by Tranter *et al*. (1997a). Precision and accuracy of the measurements is *c*. ±4%, although for the more dilute samples these values are higher.

Charge balance errors

Charge balance errors (CBE) were calculated as follows

$$\mathrm{CBE} = \frac{(\Sigma^{+} - \Sigma^{-})}{(\Sigma^{+} + \Sigma^{-})} \times 100\%$$

where Σ^{+} and Σ^{-} are the sum of the measured positive and negative equivalents respectively. The mean CBE for the borehole waters was −4%. The CBE for the majority of bulk meltwaters was < ±5%, and the

mean compositions reported below have CBE of −2% and 0% for 1993 and 1994 respectively. The CBE for supraglacial and snow samples were considerably higher, and are often >50% (largely as a result of overestimation of HCO_3^-). Concentrations of species in these waters therefore should be taken to show order of magnitude significance only.

RESULTS

Supraglacial waters and snow are very dilute. All species measured have mean concentrations <10 μmol/L (Table III), and only Ca^{2+}, SO_4^{2-}, NO_3^- (in snow) and Cl^- have mean concentrations >2 μeq/L. The mean concentrations of ions in bulk runoff were broadly similar in both sampling seasons. They are more than one or two orders of magnitude higher than those found in snow and supraglacial runoff for all ions, with the exception of Cl^- and NO_3^- (Table IV). Ca^{2+}, HCO_3^- and SO_4^{2-} are the dominant ions.

The majority of borehole waters contain more solute than bulk runoff, although some are more dilute (Table IV). Samples with measured HCO_3^- concentrations <200 μeq/L or >600 μeq/L produced charge balance errors that often were unacceptably high (> ±10%). Given the uncertainty of HCO_3^- values outside

Table III. Composition of supraglacial streams and snowmelt

Species (μeq/L)	Snow 1993–1995		Supraglacial streams	
	Mean	SD	Mean	SD
Ca^{2+}	3·8	4·6	7·5	11·8
Mg^{2+}	0·7	0·7	0·3	1·3
K^+	1·1	2·3	1·0	1·6
Na^+	0·4	1·6	1·4	1·4
SO_4^{2-}	3·3	2·6	5·6	2·8
NO_3^-	5·8	6·3	0·9	2·0
Cl^-	3·8	4·6	7·5	11·8
Si (μm)	< 0·1		< 0·1	
n	46		45	

Table IV. The chemical composition of the different subglacial water types and bulk runoff for 1993 and 1994. HCO_3^- for borehole water was estimated from charge deficit; Sd denotes standard deviation

Species (μeq/L)	Type A		Type B		Type C		Bulk runoff 1993		Bulk runoff 1994	
	Mean	Sd	Mean	Sd	Mean	Sd	Mean	Sd	Mean	Sd
Ca^{2+}	940	560	650	310	230	95	370	60	380	69
Mg^{2+}	92	65	82	23	23	22	40	8	33	9
K^+	23	10	15	8·0	33	25	14	4	12	3
Na^+	20	10	18	18	19	16	19	4	13	4
SO_4^{2-}	440	280	270	170	37	29	150	52	120	54
HCO_3^-	620	350	480	200	260	110	310	47	310	99
NO_3^-	3·7	3·6	10	9·0	1·2	1·6	5·3	2·9	5·9	5·1
Cl^-	7·9	6·1	6·3	5·1	8·2	10	3	2	6·1	6·9
Si (μm)	14	4·0	19	8·5	17	11	19	5	15	3·7
pH	7·4	0·5	7·4	0·5	8·1	0·8				
$P(CO_2)$	$10^{-2.9}$		$10^{-3.0}$		$10^{-4.0}$					
SMF	0.42		0.36		0.12					
n	≃40		≃80		≃74		≃118		≃85	

this range, the following discussion of borehole water chemistry uses HCO_3^- calculated from charge deficit, rather than measured HCO_3^-.

The subglacial waters have been divided into three types on the basis of the proportions of Ca^{2+}, SO_4^{2-} and HCO_3^- with respect to Si (Lamb *et al.*, 1995). The more concentrated borehole waters (Si >10 μmol/L) cluster into three types (Figure 2a–c), but it is a more subjective exercise for the dilute waters (Si <10 μmol/L) because the compositions of the three types converge. The three clusters also are easily identified on a scatterplot of Mg^{2+} versus Si (Figure 2d), but the clusters are not evident on a scatterplot of $(Na^+ + K^+)$ versus Si (Figure 2e). Each subglacial water type was sampled from at least two boreholes and in each of the sampling seasons (Table V).

Type A waters are most concentrated in major ions, and were sampled from Holes 39, 44 and 78. Type B waters are of intermediate concentration and were sampled from Holes 39, 51, 62, 63, 65, 67, 68 and 74. Type C waters are the most dilute (Table IV), and were sampled from Holes 31, 32, 33, 35, 38, 52, 63 and 77 (Table V). The dominant cation in all three water types is Ca^{2+} and the major anion is HCO_3^- (Table IV). The second major anion is SO_4^{2-}. Type C waters, thought to be representative of those flowing through a channel marginal zone, are equivalent to the Mode 2A waters reported in an earlier paper (Tranter *et al.*, 1997a), and Type B waters, thought to be representative of those flowing through a distributed drainage system, are similar to Mode 3 waters.

Two useful indices for describing chemical weathering environments are the partial pressure of gaseous CO_2 with which the waters are in apparent equilibrium ($p(CO_2)$) and the sulphate mass fraction (SMF). The $p(CO_2)$ gives information on the degree to which the chemical weathering environment is in equilibrium with atmospheric CO_2. Values for $p(CO_2)$, calculated from the mean pH and HCO_3^- of Type A, B and C waters (Table IV) and using $K_H = 10^{-1.12}$ mol/L^{-1} atm^{-1} and $K_1 = 10^{-6.6}$ mol/L^{-1} at 0 °C (Garrels and Christ, 1965), are $10^{-2.9}$, $10^{-3.0}$ and $10^{-4.0}$ atm respectively.

The SMF is defined as

$$\mathrm{SMF} = \frac{(SO_4^{2-})}{(SO_4^{2-}) + (HCO_3^-)}$$

where units of concentration are equivalents. Assuming that other sources of SO_4^{2-} are small, the SMF provides a crude index of HCO_3^- derived from linked sulphide oxidation and carbonate dissolution relative to other sources of HCO_3^-. The SMF of waters derived from the coupling of sulphide oxidation and carbonate dissolution should be 0·5 (Equation 4). Carbonation (Equations 1 and 2) drives values <0·5, whereas sulphide oxidation coupled to silicate weathering (Equation 5) and subglacial precipitation of carbonates drive values >0·5. The SMF values calculated from the mean concentrations of HCO_3^- and SO_4^{2-} in Type A, B and C waters (Table IV) are 0·42, 0·36 and 0·12 respectively, suggesting that sulphide oxidation coupled to carbonate dissolution cannot be the sole source of subglacial HCO_3^- (Tranter *et al.*, 1997a). The data set presented here allow the source of at least some of the additional HCO_3^- to be identified.

DISCUSSION

The type of subglacial drainage system that a borehole intercepts, the nature of water movement into and out of the borehole, and the nature of the substrate into which the borehole is drilled all have potentially important impacts on the chemical composition of meltwaters sampled at the glacier bed. The first factor determines whether or not true subglacial waters can be sampled, whereas the latter factors have the potential to impart artefacts on the water chemistry, via advection or diffusion of solutes from the overlying borehole water column or chemical weathering within the borehole environment.

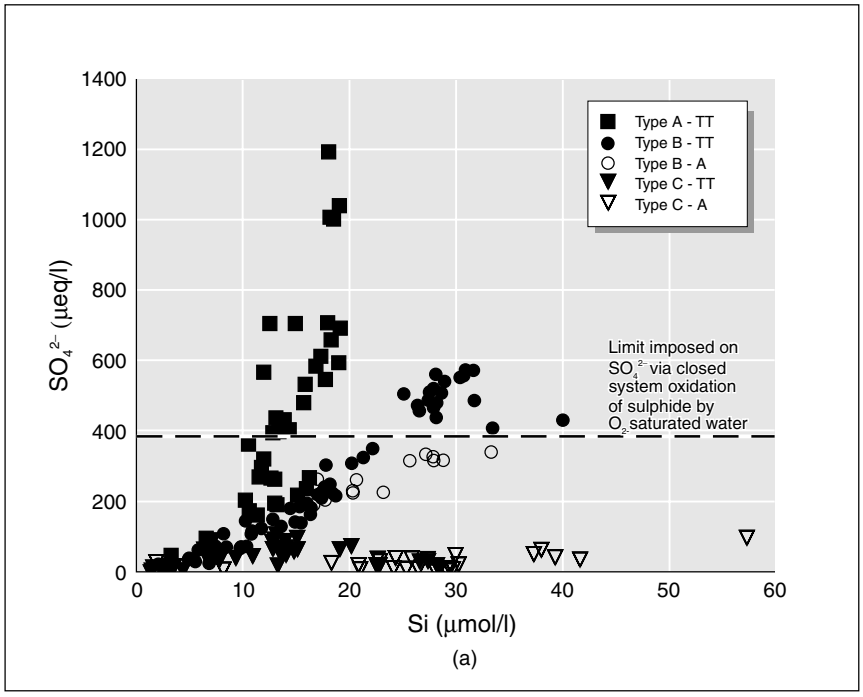

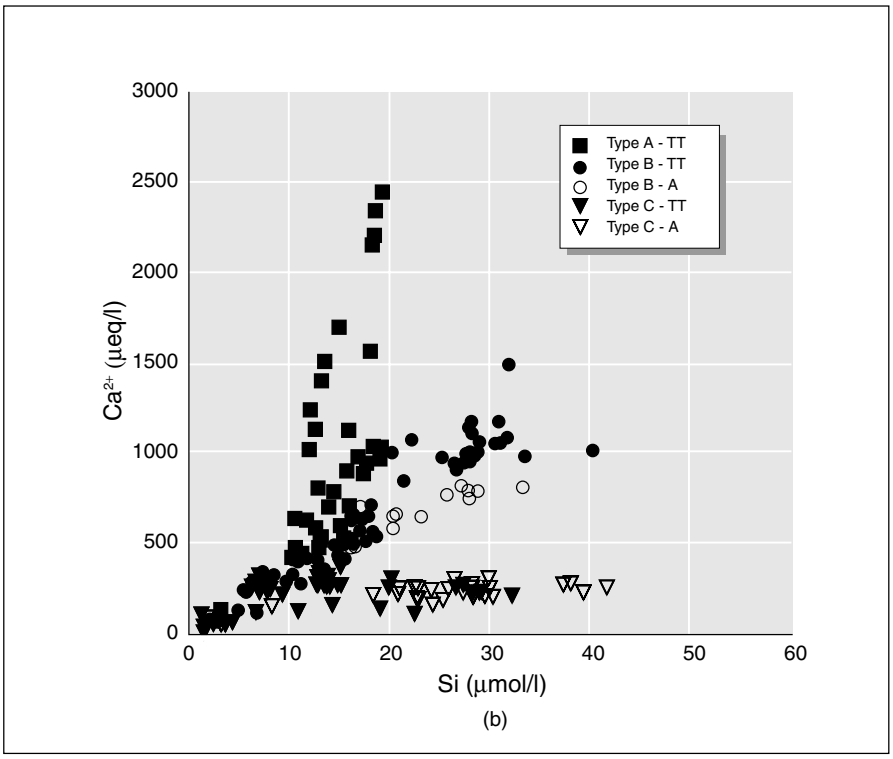

Figure 2. Scatterplots of (a) SO_4^{2-}, (b) Ca^{2+}, (c) HCO_3^- (d) Mg^{2+} and (e) $(Na^+ + K^+)$ versus Si for all borehole waters: TT denotes a true Type A, B or C water, whereas A denotes an artefact water composition

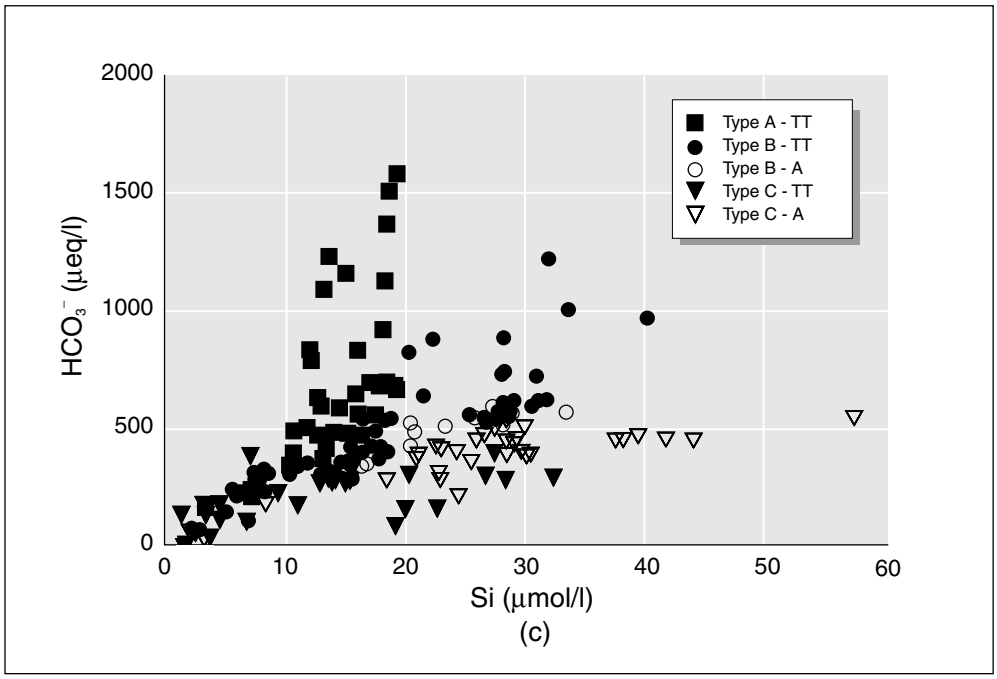

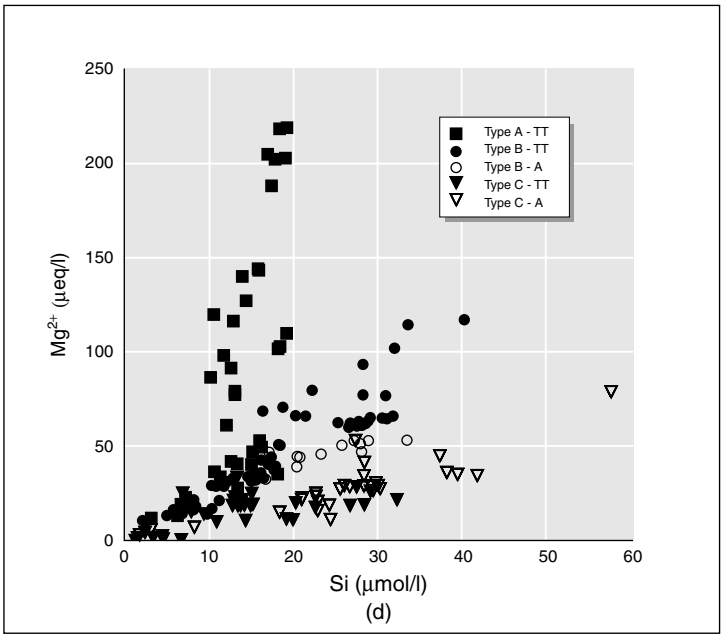

Figure 2. (*Continued*)

The hydrology of the boreholes and borehole water types

Boreholes drilled to the glacier bed can be classified as either connected or unconnected (Waddington and Clarke, 1994). Unconnected holes that reach the bed do not establish a connection with the subglacial

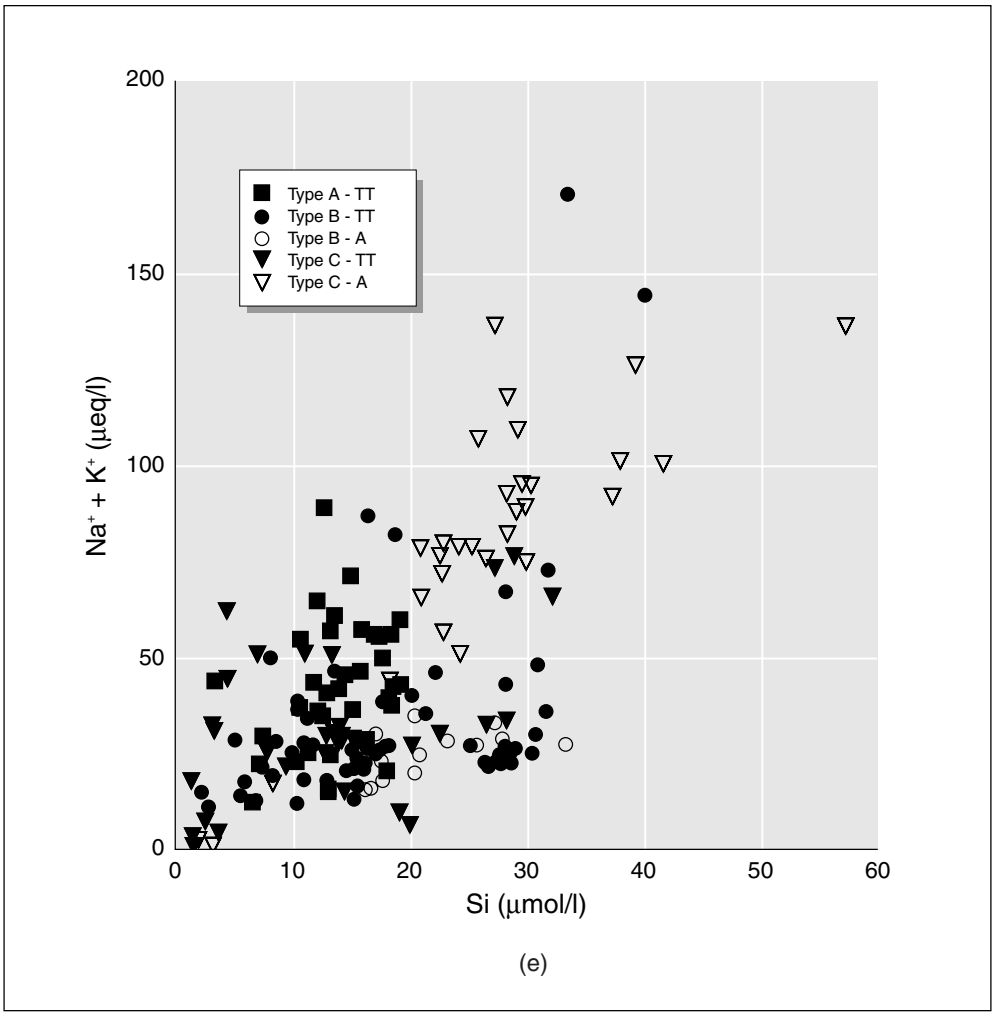

Figure 2. (*Continued*)

drainage system. These holes remain water-filled and there is little change in the borehole water chemistry (Tranter *et al*., 1997a). Analysis of water level (WL) and electrical conductivity stratification (ECS) variations suggests that Holes 31, 33, 38, 52, 65 and 77 were unconnected throughout the sampling period (Table V). Connected holes, on the other hand, exhibit fluctuating WL and ECS. They may be predominantly high- or low-standing with respect to daily minimum water levels (Smart, 1996). Connections to the subglacial drainage system may be via the base of the borehole and/or via englacial channels that intersect the borehole. The type of connection is inferred from the combination of WL and ECS variations (Gordon *et al*., 1998). Basal connections are inferred when relatively concentrated water enters via the base and both ECS and WL rise (Figure 3, Hole 74). Care must be taken in classifying concentrated basal waters if the water level varies but the ECS does not, since this may indicate that the base is hydrologically isolated by englacial connections higher up the borehole (Figure 3, Hole 39). The basal water chemistry may then carry an imprint of the borehole weathering environment.

Englacial connections carrying concentrated water are inferred when concentrated waters appear some distance from the bed, but are not present at the base of the hole (Figure 3, Hole 44). Holes may have both

Table V. Summary of borehole chemical characteristics and the degree of connectivity to the subglacial drainage system. The chemical composition of the different water types is summarized in Table IV: TT denotes the water composition is true (i.e. representative of those in the subglacial drainage system), whereas A denotes it is an artefact of the borehole chemical weathering environment. Refer to Figure 3 for details of borehole water level and electrical conductivity variations

Water Type	Hole	True type or artefact	Nature of subglacial connection	Year and sampling Period (JD)
A	39[a]	TT	Englacial connection *c*. 10 m ab	1993 223–228
	44	TT	Englacial connection *c*. 50 m ab	1993 200–208
	78	TT	Englacial connection *c*. 20 m ab	1994
			and weaker basal connection	234–242
B	51	TT	Basal connection	1993 225–235
	62	TT	Basal connection	1994 203–214
	67	TT	Basal connection	1994 221–242
	68	TT	Basal connection	1994 222–235
	74	TT	Basal and englacial connections	1994 224–238
	65	A	Unconnected	1994 208–214
C	32	TT	Basal connection	1993 222–225
	35	TT	Basal connection	1993 210–213
	63[b]	TT	Formerly englacially connected. Became progressively basally connected	1994 208–235
	31	A	Unconnected	1993 211–212
	33	A	Unconnected	1993 213–222
	38	A	Unconnected	1993 210–213
	52	A	Unconnected	1993 225–235
	77	A	Unconnected	1994 231–240

[a] Hole 39 contained predominantly Type A water, but also contained Type B water periodically during the later stages of sampling.
[b] Hole 63 contained Type C waters in the earlier stages of sampling, but contained Type B waters when the basal connection was established.

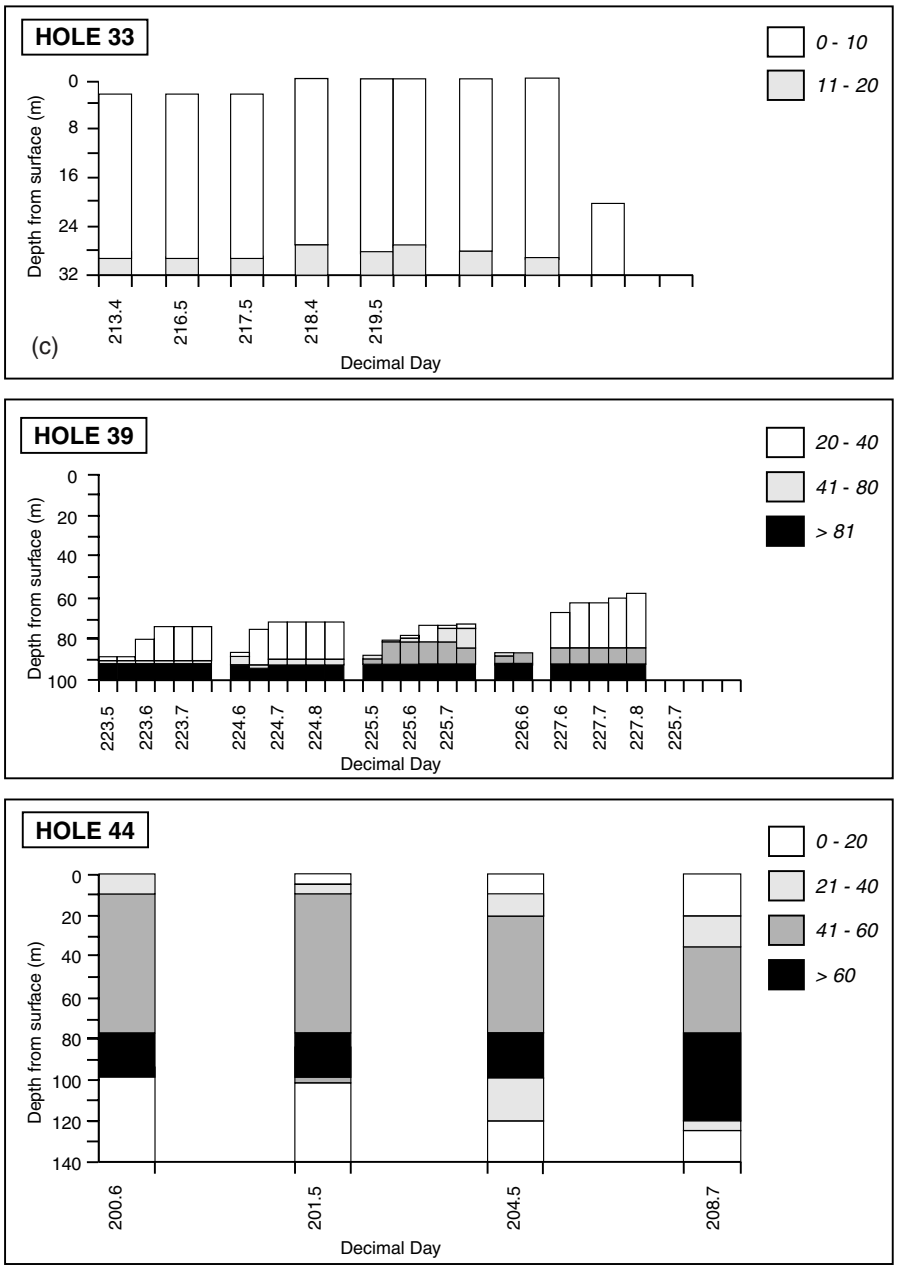

Figure 3. Water level and electrical conductivity stratification over time in all boreholes sampled. The legend in each figure shows the electrical conductivity, which is in units of μS/cm. Gaps in these records denote that no data are available, rather than that the boreholes ran dry

basal and englacial connections (Figure 3, Hole 78), the relative importance of which may change during the sampling period (Figure 3, Hole 67). It is assumed that concentrated waters issuing from englacial connections originated at the bed because it is difficult to imagine significant englacial chemical weathering environments with large quantities of reactive debris. The inferred hydrology of each borehole sampled is summarized in Table V.

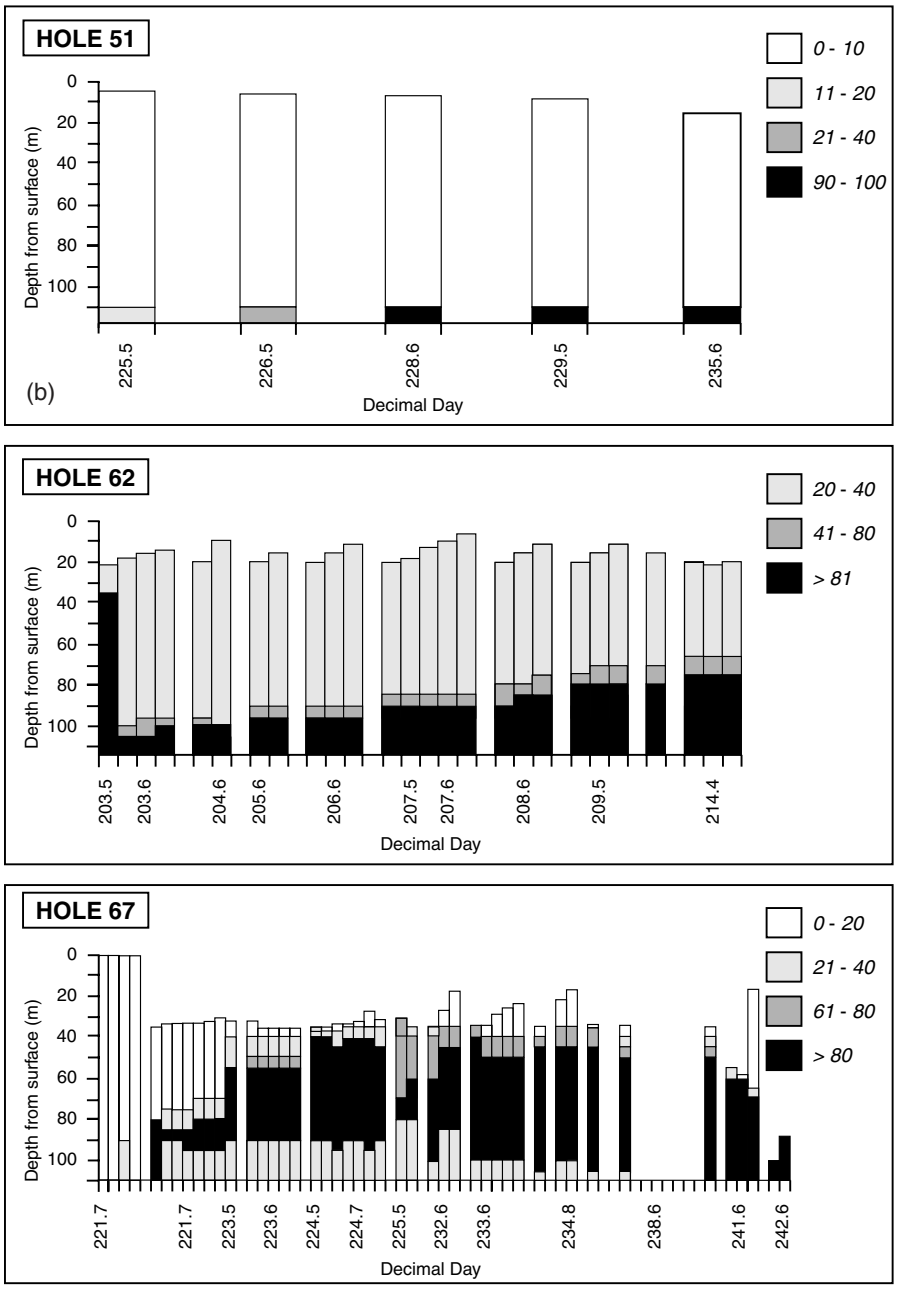

Figure 3. (*Continued*)

Type A waters are associated with holes that are englacially connected (Table V). The concentrated waters flowing through these englacial connections must have been formerly at the bed in a drainage pathway that has not been accessed by the other connected boreholes. All Type A waters were clear, implying that they had insufficient energy to entrain sediment (Stone and Clarke, 1996). Two of the three holes (Holes 39 and 78) are close to the predicted location of a major subglacial channel (Sharp *et al*., 1993; Figure 1b). The third (Hole 44) lies just outside the *variable pressure axis* (Hubbard *et al*., 1995) in which there are diurnal

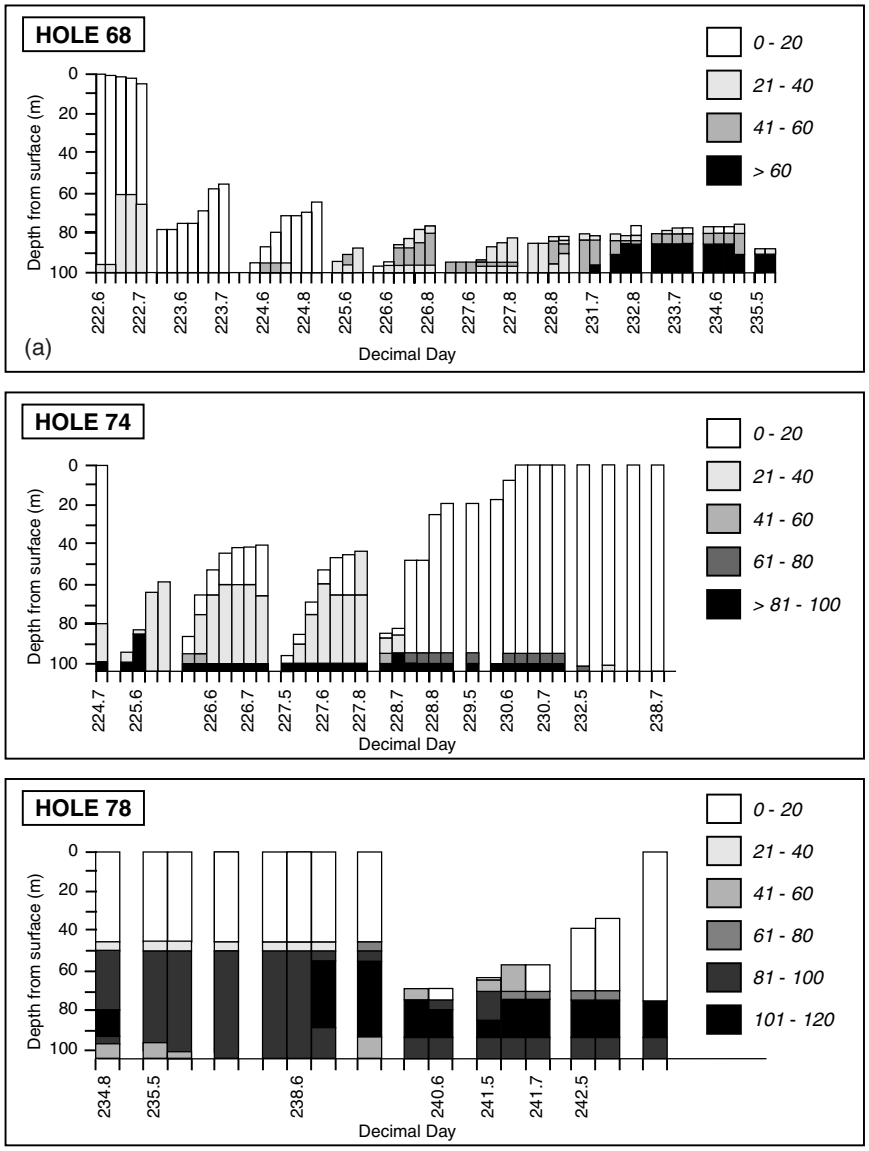

Figure 3. (*Continued*)

variations in water level. Type B waters are found usually in holes with basal connections that are located in the variable pressure zone. By contrast, most Type C waters are found in unconnected holes, although some are from basally connected holes.

Solute acquisition within the borehole environment

It is possible that some of the sampled water chemistries were generated by chemical weathering in the borehole environment, rather than in the natural subglacial drainage system. Glacial debris may be suspended in the borehole during drilling or reaming, and may contribute solute to dilute borehole waters by carbonation reactions (Tranter *et al*., 1997a) or carbonate hydrolysis (see below). The borehole water chemistries presented here have been designated as either 'true' or 'artefact' on the basis of the WL and ECS variations in the

boreholes from which they were sampled. Chemistries are designated as 'true' only where there is reasonable evidence that waters were derived directly from the glacier bed via basal or englacial connections, so that it is also reasonable to assume that most solute was acquired in the subglacial drainage system. Otherwise, the water chemistry is designated as 'artefact'. Table V indicates which holes contain 'true' subglacial waters. It should be noted that the concentration of ions in true subglacial waters may be diminished by mixing with dilute waters that invade the subglacial drainage system from the boreholes.

First-order controls on subglacial water chemistry

All subglacial waters that were sampled (i.e. all three water types ensemble), plus some collected during 1992 (Tranter *et al.*, 1997a), will be used to determine the first-order controls on their chemical composition.

True and artefact water chemistries. Both true and artefact water chemistries can be used to define the nature of subglacial chemical weathering reactions. Artefact water compositions show the direction of possible subglacial chemical weathering reactions, because subglacial debris has interacted with icemelt from drilling or surface sources, albeit in a borehole rather than in a subglacial environment. Hence, for discussion of the first-order controls on chemical weathering at the bed of Haut Glacier d'Arolla, artefact water chemistries are included in the data set. True Type C waters with high Si concentrations were not collected during 1993 and 1994, but were sampled during 1992 (Tranter *et al.*, 1997a). These latter samples were combined with the 1993–1994 data sets to give the broadest coverage of subglacial water types possible. There is usually overlap between true and artefact water chemistries (Figure 2), confirming both our assertion that chemical weathering in the borehole environment can be similar to that at the glacier bed and that we have been conservative in our classification of true type waters. There is overlap also in the composition of the artefact Type C waters collected during 1993 and 1994 and the true Type C waters collected during 1992 (Figure 2). Figure 2 shows that all waters with SO_4^{2-} concentrations greater than 400 μeq/L are true type.

Evidence for carbonate hydrolysis. There is a good linear association between $(Ca^{2+} + Mg^{2+})$ and SO_4^{2-}, $(Ca^{2+} + Mg^{2+})$ and HCO_3^-, and HCO_3^- and SO_4^{2-} (Figure 4a, b and c), although clearly there are outliers on the HCO_3^- versus SO_4^{2-} scatter plot (see below). The r^2 values are 0·90 ($n = 191$), 0·91 ($n = 188$) and 0·71 ($n = 195$) respectively. The linear associations between the major ions can arise in two ways. First, there may be dilution of a concentrated component (a quasi-mixing control; Lamb *et al.*, 1995), for example, when concentrated waters from the distributed drainage system invade the channel and channel margin zone during periods of low diurnal discharge and mix with more dilute water. Second, there may be linkages between the dissolution of different minerals, such that the dissolution of the least reactive mineral determines the concentration of all species (a quasi-kinetic control, Lamb *et al.*, 1995). It is probable that both controls exist in the subglacial drainage system that was sampled.

The slopes of best-fit regression equations for $(Ca^{2+} + Mg^{2+})$ and HCO_3^- versus SO_4^{2-} (Table VI) suggest that these ions are acquired by the subglacial waters in the ratio $1{\cdot}73(\pm 0{\cdot}03) : 0{\cdot}78(\pm 0{\cdot}04) : 1$. This is close to the ratio that would arise if carbonate dissolution and sulphide oxidation alone were a first-order control on the water chemistry (Equation 4), namely 2 : 1 : 1 in units of equivalents. This reaction cannot account for all solute acquisition in the subglacial environment, because the best-fit regression equations of $(Ca^{2+} + Mg^{2+})$ and HCO_3^- versus SO_4^{2-} have large positive intercepts (178 ± 9 and 225 ± 10 μeq/L respectively). This suggests that the subglacial waters have acquired $(Ca^{2+} + Mg^{2+})$ and HCO_3^- concentrations of *c.* 180–230 μeq/L prior to their acquisition of SO_4^{2-}. A more accurate statement is that Ca^{2+}, Mg^{2+} and HCO_3^- initially are acquired more rapidly than SO_4^{2-}, as waters with <100 μeq/L SO_4^{2-} show non-linearity in the association between the other ions and SO_4^{2-} (Figure 4a and b). The relatively rapid acquisition of Ca^{2+}, Mg^{2+} and HCO_3^- with respect to SO_4^{2-} has been observed in meltwaters from Glacier de Tsanfleuron, which overlies carbonate bedrock (Fairchild *et al.*, 1994), although the 'zero-SO_4^{2-}' concentrations of Ca^{2+} and HCO_3^- were smaller. Table VI also shows the best-fit regression equations of $(Ca^{2+} + Mg^{2+})$ and HCO_3^- versus SO_4^{2-}

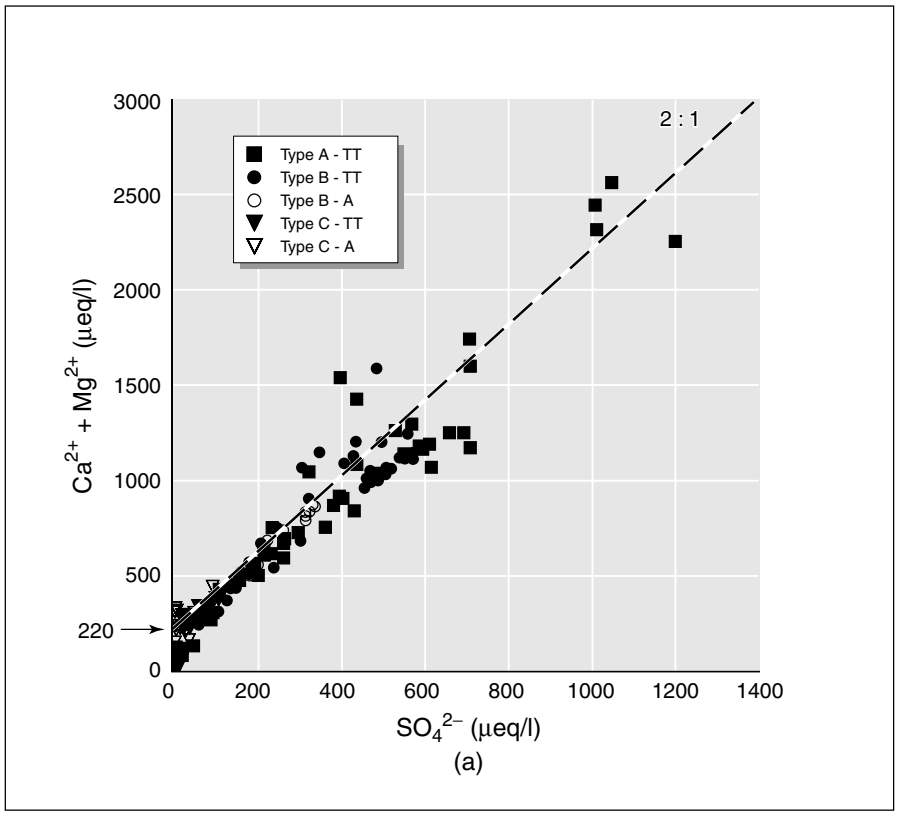

Figure 4. Scatterplot of (a) (Ca^{2+} and Mg^{2+}) versus $SO_4{}^{2-}$, (b) $HCO_3{}^-$ versus $SO_4{}^{2-}$, (c) (Ca^{2+} and Mg^{2+}) versus $HCO_3{}^-$, for all borehole waters, (d) ($Na^+ + K^+$) versus $SO_4{}^{2-}$, (e) ($Na^+ + K^+$) versus $HCO_3{}^-$ and (f) (Ca^{2+} and Mg^{2+}): ($Na^+ + K^+$) versus ionic strength: TT denotes a true Type A, B or C water, whereas A denotes an artefact water composition

for $SO_4{}^{2-} > 100$ µeq/L. There is a better agreement between the intercepts (232 ± 13 cf. 217 ± 12 µeq/L). We can therefore reasonably assume that *c*. 220 µeq/L of ($Ca^{2+} + Mg^{2+}$) and $HCO_3{}^-$ are acquired during the initial stages of rock–water interaction in the subglacial environments that we have sampled, during which time relatively little $SO_4{}^{2-}$ is acquired. These environments presumably are water-full, because none of the boreholes ran dry, and therefore are out of contact with atmospheric CO_2. Hence, this solute can have been acquired only from dissolution of glacial till, rock flour or bedrock because no atmospheric source of solute is available. This suggests that the meltwaters were involved initially in carbonate hydrolysis (Equation 6), which does not require a proton source and is rapid (Plummer and Wigley, 1976). Similar reactions occur when silicates such as feldspars are first wetted (Equation 7; Garrels and Howard, 1959).

The theoretical solubility of calcite in distilled water, initially saturated with air, at 0 °C is *c*. 250 µeq/L of Ca^{2+}, balanced by *c*. 160 µeq/L of $HCO_3{}^-$, *c*. 80 µeq/L of $CO_3{}^{2-}$ and *c*. 10 µeq/L of OH^- (after Garrels and Christ, 1965). This solution has a high pH (*c*. 10) and a low pCO_2 (*c*. 10^{-6} atm). The theoretical values for Ca^{2+} and ($HCO_3^- + CO_3{}^{2-}$) are close to the intercepts for the best-fit lines of ($Ca^{2+} + Mg^{2+}$) and $HCO_3{}^-$ versus $SO_4{}^{2-}$. This, together with the kinetic favourability of the reaction during the initial stages of rock–water contact (Plummer and Wigley, 1976), suggests that hydrolysis of the trace carbonate component of subglacial sediments is the dominant initial rock–water reaction that occurs in water-filled, subglacial chemical weathering environments. Subsequent re-equilibration of the resulting solution with atmospheric CO_2 following emergence of the waters at the glacier terminus or during transit in partially full subglacial

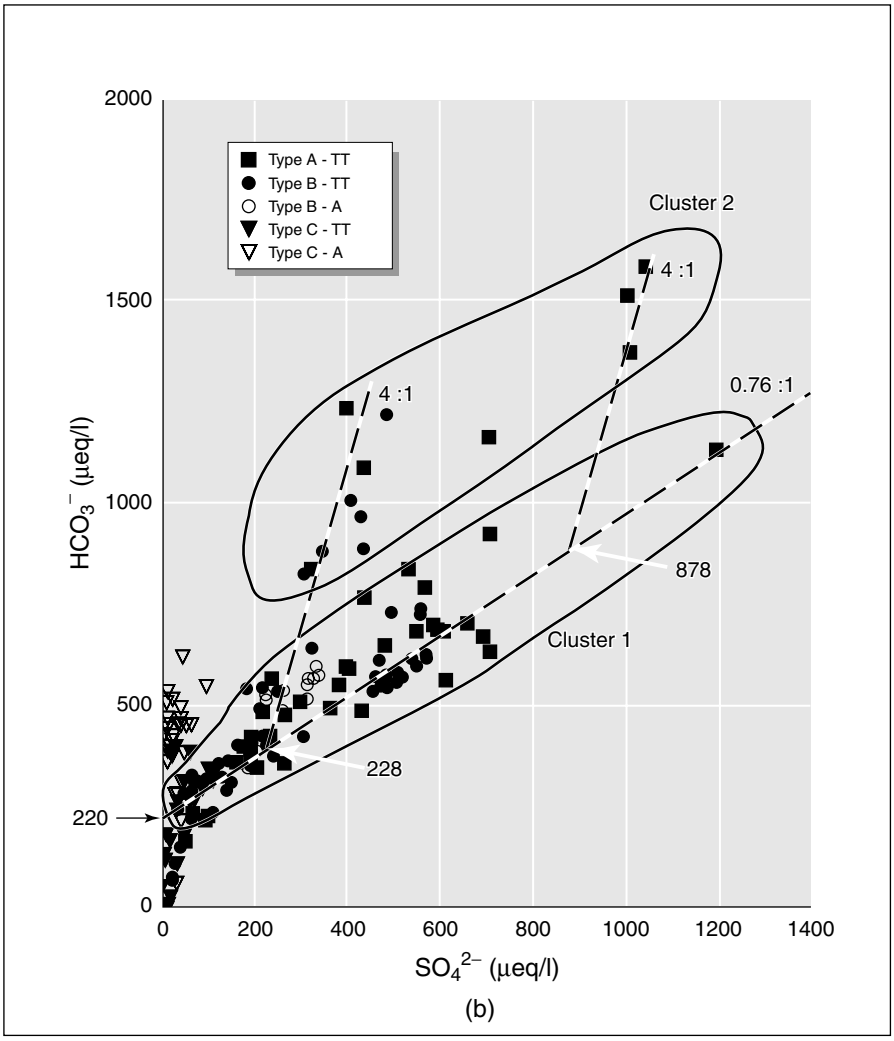

Figure 4. (*Continued*)

channels produces a solution with characteristics similar to those produced by carbonation of carbonate (Equation 2).

The range of measured $(Ca^{2+} + Mg^{2+})$ and HCO_3^- concentrations in low (<100 µeq/L) SO_4^{2-} waters (Figure 4b) is 0–500 µeq/L. Measured values of $(Ca^{2+} + Mg^{2+})$ and HCO_3^- that are $<c$. 250 µeq/L suggest either that some of the subglacial debris contains very little carbonate (S. H. Bottrell, personal communication) or that waters have not yet reached equilibrium with the carbonate, because the rate of carbonate hydrolysis slows appreciably as equilibrium is approached (Plummer and Wigley, 1976). Values of $(Ca^{2+} + Mg^{2+})$ and HCO_3^- that are >250 µeq/L, which are associated mainly with artefact water types, require additional reactions to carry Ca^{2+} concentrations beyond the initial carbonate hydrolysis phase. These are likely to include coupled sulphide oxidation and carbonate/silicate dissolution (Equations 4 and 5), the microbial oxidation of organic carbon (Equation 3) and the carbonation of silicates and carbonates (Equations 1 and 2) in subglacial debris, with the latter utilizing CO_2 that diffuses down the borehole water column. Subglacial microbial oxidation of organic carbon has been inferred from $\delta^{13}C(HCO_3^-)$ variations in bulk runoff (−1·7 to −8·3 ‰)

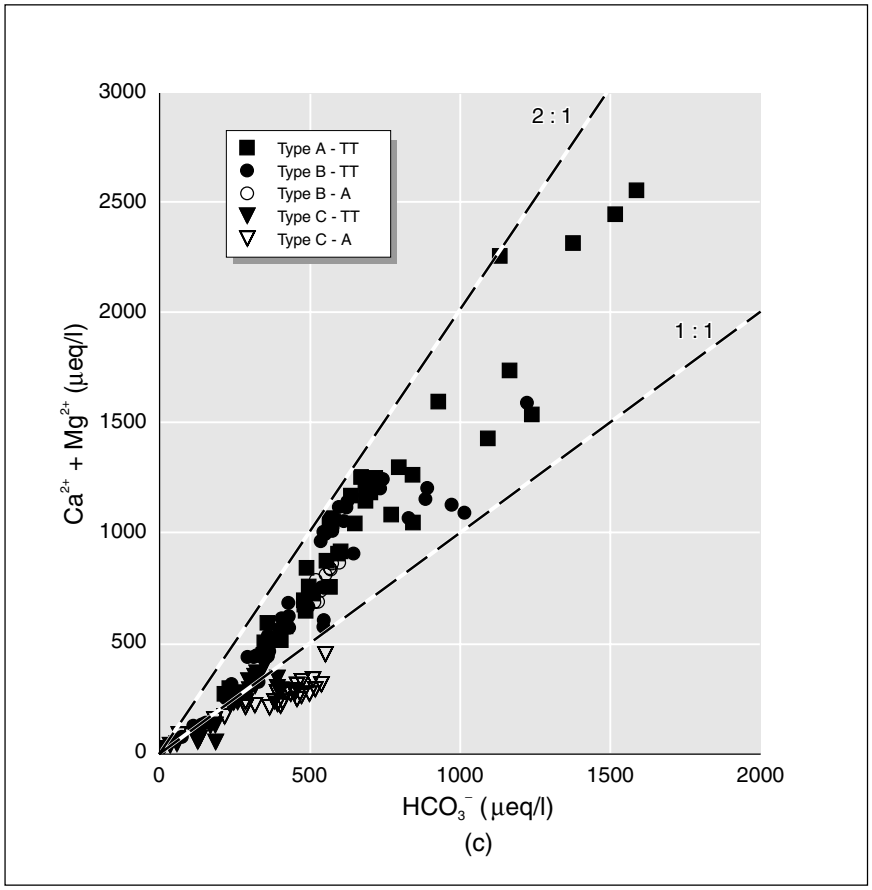

Figure 4. (*Continued*)

and the relatively ^{13}C-depleted values ($-7{\cdot}8$ and $-10{\cdot}2$ ‰) of the two subglacial meltwaters that have been analysed at Haut Glacier d'Arolla to date (S. H. Bottrell, unpublished data).

Cation exchange/silicate hydrolysis effects on the proportional cation concentration of dilute subglacial waters

Figure 4c shows that many of the more dilute meltwaters ($HCO_3^- < 500$ µeq/L) contain ratios of $(Ca^{2+} + Mg^{2+}) : HCO_3^-$ that are $<1:1$. This is surprising, because carbonate hydrolysis should produce waters with ratios of *c*. 1 : 1. The excess HCO_3^- in these waters is balanced by Na^+ and K^+. It is unlikely that Na–K-carbonates are found in the bedrock. Instead, it is more likely that rapid cation exchange is occurring, and that some of the Ca^{2+} and Mg^{2+} liberated from carbonate hydrolysis is exchanged for Na^+ and K^+ held on surface exchange sites on the subglacial debris. Figure 4f shows the ratio of $(Ca^{2+} + Mg^{2+}) : (Na^+ + K^+)$ as a function of ionic strength. Exchange surfaces preferentially adsorb divalent cations at low ionic strength (Stumm and Morgan, 1996). This appears to be the case for the borehole water samples, as the ratio of $(Ca^{2+} + Mg^{2+}) : (Na^+ + K^+)$ in solution is lowest for waters with low ionic strength. Hence, we believe that ion exchange has an impact on the concentration of low ionic strength subglacial waters, removing Ca^{2+} and Mg^{2+} from solution and replacing them with Na^+ and K^+.

Not all of the Na^+ and K^+ initially released to solution can be derived from cation exchange, as some must be released by silicate hydrolysis (Equation 7). Silicate hydrolysis probably helps to explain why the initial

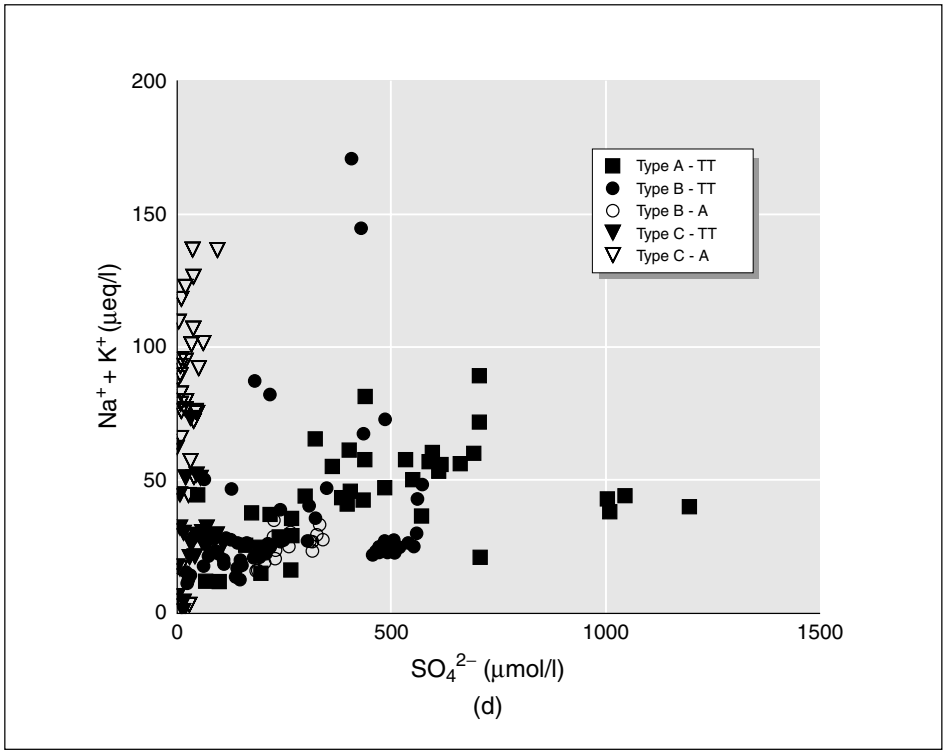

(d)

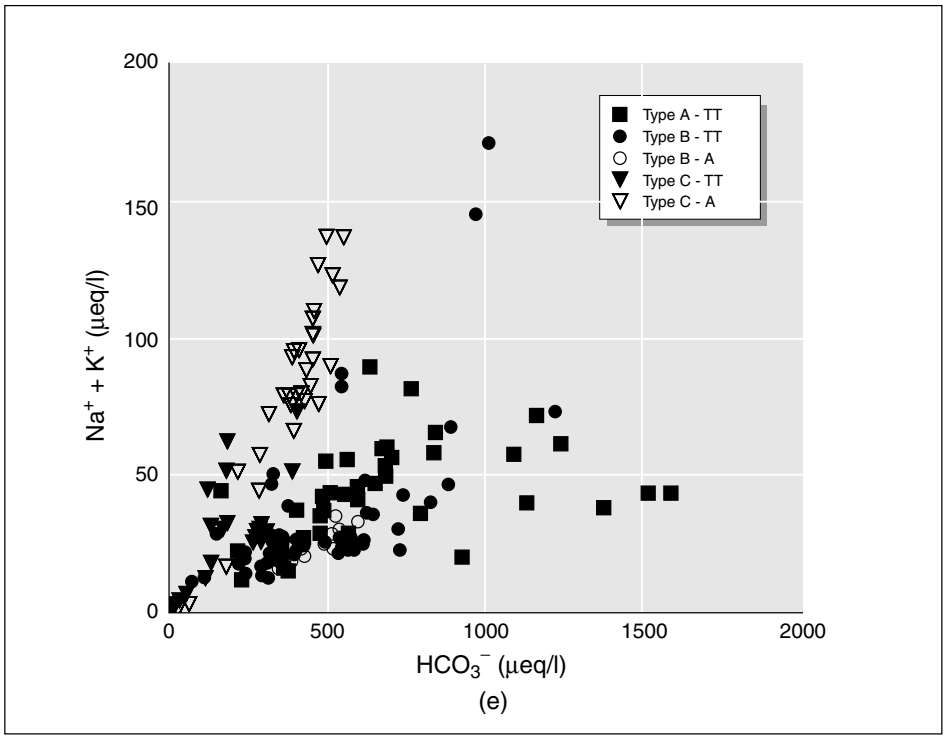

(e)

Figure 4. (*Continued*)

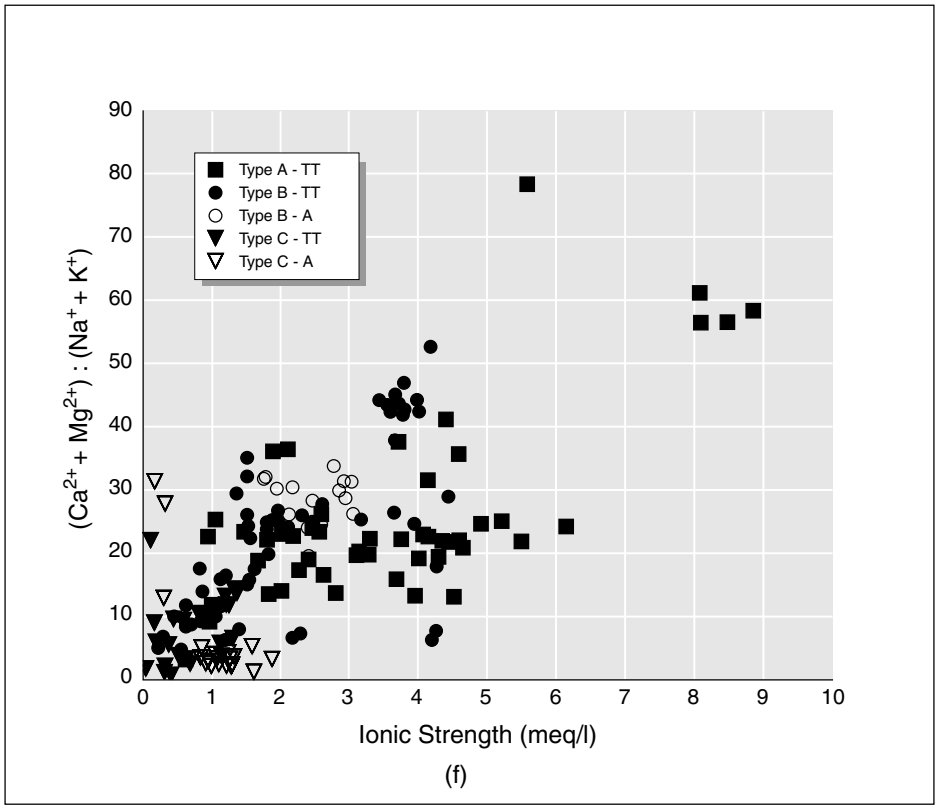

Figure 4. (*Continued*)

release of divalent ions by carbonate hydrolysis is lower than the theoretical value of 250 μeq/L. Silicate hydrolysis also increases the pH, thereby decreasing the amount of carbonate that initially can be dissolved in a closed system (Garrels and Christ, 1965).

Linkage between sulphide oxidation, carbonate and silicate dissolution. Given that the dominant initial reactions in the subglacial drainage system are carbonate–silicate hydrolysis and cation exchange, the next set of reactions is likely to be sulphide oxidation and carbonate–silicate dissolution (Equations 4 and 5), because subglacial sources of CO_2 are restricted and carbonation will be limited. All subglacial waters that were sampled were undersaturated with respect to calcite. Figure 4b reveals that there are two main data clusters for $SO_4^{2-} > 100$ μeq/L. The lower cluster, containing most of the data, will be examined first. Processes giving rise to the second cluster are discussed later.

The best-fit regression equations for the lower cluster are given in Table IV (the outliers are mostly in the second cluster). The slopes of the regression equations suggest that following carbonate hydrolysis, 1·68 ± 0·03 μeq ($Ca^{2+} + Mg^{2+}$) and 0·76 ± 0·03 μeq of HCO_3^- are acquired along with each μeq of SO_4^{2-}, rather than the 2 μeq/L of ($Ca^{2+} + Mg^{2+}$) and 1 μeq/L of HCO_3^- for each μeq/L of SO_4^{2-} that is expected if sulphide oxidation and carbonate dissolution are the only additional reactions (Equation 4). Hence, *c*. 76% (0·76 ± 0·03 units) of the protons liberated from sulphide oxidation are used to dissolve carbonates. A crude estimate of the proportions of divalent ions derived from silicate and carbonate weathering can be derived as follows. Assuming that all HCO_3^- is derived from Ca and Mg carbonates (0·76 × 2 = 1·52 units), and that any stoichiometric excess ($Ca^{2+} + Mg^{2+}$) is derived from silicates (1·68 − 1·52 = 0·16 units), the ratio of ($Ca^{2+} + Mg^{2+}$) derived from silicate and carbonate sources is 0·16 ± 0·04 : 1·52 ± 0·04. This calculation does

Table VI. Best-fit simple linear regression equations for borehole waters, using sulphate (or $SO_4^{2-} > 100$ μeq/L) as the independant variable. Analysis was conducted using all samples and each individual water type. Each cell contains, from top to bottom, the regression slope, the intercept, the R^2 value, the number of samples used in the analysis and the number of outliers. Outliers were defined as those points lying outside the 95% prediction limits on the initial regression analysis

Versus SO_4^{2-}	All	Type A	Type B	Type C	Versus SO_4^{2-} ($SO_4^{2-} > 100$ μeq/L)	All
Ca^{2+}	1·73 ± 0·03 160 ± 8 $R^2 = 0{\cdot}975$ $n = 176$ $o = 16$	1·87 ± 0·12 76 ± 64 $R^2 = 0{\cdot}925$ $n = 42$ $o = 1$	1·73 ± 0·05 173 ± 15 $R^2 = 0{\cdot}976$ $n = 74$ $o = 3$	1·91 ± 0·23 155 ± 11 $R^2 = 0{\cdot}723$ $n = 66$ $o = 6$	$Ca^{2+} + Mg^{2+}$	1·68 ± 0·03 232 ± 13 $R^2 = 0{\cdot}968$ $n = 89$ $o = 13$
$Ca^{2+} + Mg^{2+}$	1·87 ± 0·03 178 ± 9 $R^2 = 0{\cdot}976$ $n = 182$ $o = 9$	1·98 ± 0·10 129 ± 52 $R^2 = 0{\cdot}955$ $n = 41$ $o = 2$	1·83 ± 0·05 189 ± 17 $R^2 = 0{\cdot}973$ $n = 74$ $o = 3$	2·00 ± 0·28 173 ± 14 $R^2 = 0{\cdot}661$ $n = 68$ $o = 4$	HCO_3^-	0·76 ± 0·03 217 ± 12 $R^2 = 0{\cdot}870$ $n = 94$ $o = 13$
HCO_3^-	0·78 ± 0·04 225 ± 10 $R^2 = 0{\cdot}851$ $n = 185$ $o = 10$	1·13 ± 0·08 104 ± 42 $R^2 = 0{\cdot}904$ $n = 43$ $o = 2$	0·83 ± 0·04 191 ± 13 $R^2 = 0{\cdot}919$ $n = 73$ $o = 6$	1·53 ± 0·47 214 ± 23 $R^2 = 0{\cdot}367$ $n = 69$ $o = 2$		

not take into account the confounding effects of ion exchange in subglacial sediments (Wadham *et al.*, 1998), which tends to diminish divalent ion concentrations. Given the errors associated with this calculation, *c*. 11% of the Ca^{2+} and Mg^{2+} in the lower cluster waters is derived from silicate weathering following carbonate hydrolysis, and *c*. 10% of the protons derived from sulphide oxidation are used to dissolve Ca–Mg silicates.

Figure 4d shows that variable amounts of (Na^+ and K^+) are released from the chemical weathering of silicates (Equation 5 and Figure 2e) for each unit of SO_4^{2-} liberated from sulphide oxidation. The main cluster has a slope of *c*. 0·1. Hence, *c*. 10% of the protons liberated by sulphide oxidation are used to chemically weather Na and K feldspars. We have now accounted for the sink of *c*. 100% (i.e. 76 + 10 + 10%) of the protons liberated by sulphide oxidation. Overall, a crude ratio of the relative amounts of carbonate and silicate dissolution arising from sulphide oxidation is therefore *c*. 76 : 20 or *c*. 4 : 1. This compares with the global terrestrial average rate of *c*. 1·3 : 1 (Holland, 1978), confirming that waters at Haut Glacier d'Arolla preferentially dissolve carbonates from the bedrock with respect to silicates, despite the bedrock being predominantly silicate.

Sulphide oxidation—the need for an additional subglacial oxidizing agent. It was shown above that the amount of SO_4^{2-} that could be liberated by closed-system oxidation of sulphide is *c*. 386 μeq/L, assuming that the water is saturated initially with O_2 at 0 °C and that there are no other subglacial sources or sinks of O_2. The value of 386 μeq/L should be considered an upper limit, because meltwaters generated at higher altitudes on the glacier have lower saturated O_2 contents (as low as 85% of the value at the terminus) and supraglacial snow- and icemelt may be undersaturated with respect to atmospheric pO_2 (values as low as 34% saturation have been recorded; Brown *et al.*, 1994b). Hence, some supraglacial waters have an oxygen content that will give rise to a maximum SO_4^{2-} concentration of only *c*. 30 μeq/L. Many subglacial waters have $SO_4^{2-} > 400$ μeq/L, particularly Type A waters (Figure 4a). This requires either that there is a subglacial source of O_2 or that there is another subglacial oxidizing agent. These possibilities are discussed further below.

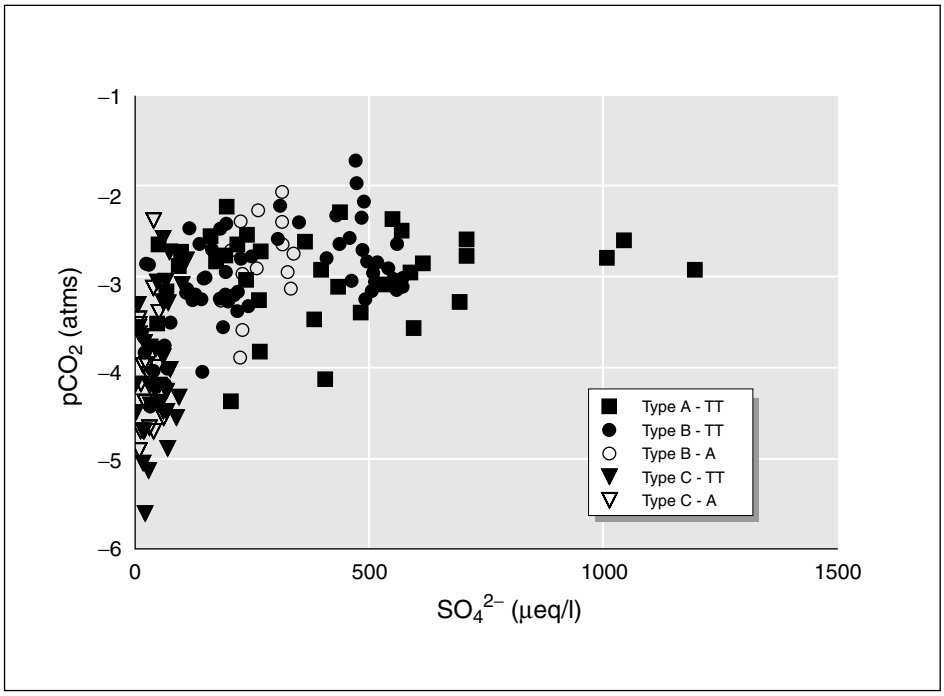

Figure 5. Scatterplot of $p(CO_2)$ versus SO_4^{2-} for all borehole waters: TT denotes a true Type A, B or C water, whereas A denotes an artefact water composition

Controls on Si concentrations. The source of Si is either from the dissolution of quartz polymorphs or other silicate minerals. The dissolution of Si from quartz polymorphs does not require a proton source, as shown by Equation (8). The rate of quartz dissolution is several orders of magnitude slower than that of Si dissolution from silicates (Lerman, 1979), as illustrated in Equations (7), (8) and (9) which are written as hydrolysis reactions. Hence, silicate dissolution is the more likely source of dissolved Si.

Carbonate and silicate hydrolysis are the kinetically favourable reactions in a multimineralic mixture of silicates and carbonates, and congruent dissolution of silicates is likely to be inhibited by the resulting high pH. However, the high pH may promote incongruent dissolution of Si from silicates (Knauss and Wolery, 1986; Brady and Walther, 1989) and enhanced dissolution of Si from silica (Gratz and Bird, 1993). The possible impact of hydrolysis on dissolved Si concentrations in subglacial meltwaters is discussed further below.

Summary of principal chemical weathering reactions. The above discussion has shown that carbonate–silicate hydrolysis and cation exchange of divalent ions in solution for monovalent ions on surface exchange sites are the initial reactions that most waters undergo on contact with glacial debris at the bed. Thereafter, sulphide oxidation dissolves carbonates and silicates in a crude ratio of 4 : 1. The chemical weathering reactions responsible for controlling the different water types can now be examined with this backdrop in mind.

Controls on the chemical composition of Type A waters

Type A waters were sampled in three high-standing holes. No similar waters were sampled during 1992 (Tranter *et al.*, 1997a). Type A waters are concentrated and associated with englacial borehole connections, which implies that water has moved from the bed under pressure, perhaps because the basal drainage system

is inefficient in this area. The negligible suspended sediment content of the waters suggests a slow moving hydrological flow path. The main chemical features of these waters are the relatively high concentrations of major ions (Table III) and the relatively low concentrations of Si (Figure 2). The highest concentration of SO_4^{2-}, *c*. 1200 μeq/L, is approximately three times the maximum concentration that can be obtained from the closed-system oxidation of sulphides by oxygen (see above). The $P(CO_2)$ of the waters are often above atmospheric levels (Figure 5). The following discussion attempts to explain these characteristics.

There are four potential means of generating SO_4^{2-} concentrations >386 μeq/L. First, there is substantial refreezing of subglacial waters. Second, there could be a subglacial source of O_2 (e.g. from gas bubbles in ice along flow-path walls). Third, there is an alternative source of SO_4^{2-} (e.g. gypsum), and fourth, there is an additional mechanism of oxidizing sulphide in subglacial environments. Of these possibilities, it seems unlikely that substantial refreezing occurs at the base of this temperate glacier, unless it is associated with regelation. Regelation waters might acquire solute en route from the stoss to the lee side of bedrock obstacles and precipitate salts on refreezing (Hallet, 1976). Regelation waters containing Ca^{2+}, HCO_3^- and SO_4^{2-} as the principal ions have the potential to precipitate first carbonate and then gypsum. The ions in any secondary gypsum precipitate can readily redissolve in subsequent subglacial waters that they may encounter, providing a source of SO_4^{2-} (and Ca^{2+}) that is independent of both oxygen and proton sources (Equation 11).

Table VI and Figure 4a show that the increase in the Ca^{2+} and SO_4^{2-} concentrations of Type A waters is in the ratio of *c*. 2, rather than *c*. 1 that would be anticipated for gypsum dissolution (Equation 11). Hence, it is unlikely that secondary gypsum dissolution is the source of the high SO_4^2 concentrations in these Type A waters.

Both regelation and melting of ice walls along subglacial flow paths may release O_2 to subglacial chemical weathering environments, dependent on the bubble concentration and gas content of the melting ice. This may promote additional sulphide oxidation. Hence, waters in the vicinity of bedrock obstacles where regelation is taking place may receive a subglacial supply of O_2 (and CO_2) that is dependent on the composition and concentration of gas bubbles in the basal ice.

Biogeochemically plausible means of generating high SO_4^{2-} concentrations require that Fe^{2+} and Fe^{3+} ions, from sources such as silicates and Fe^{III} oxyhydroxides, participate in sulphide oxidation. There is firm evidence that microbial activity occurs under Haut Glacier d'Arolla (Sharp *et al.*, 1999). Microbial activity is likely to catalyse sulphide oxidation (Singer and Stumm, 1970) and to oxidize organic carbon (Equation 3). Both reactions lower the partial pressure of O_2 in solution, and may promote suboxic conditions where the continued oxidation of sulphides is achieved by utilizing NO_3^-, Mn^{IV} and Fe^{III} as oxidizing agents (Drever, 1988). Fe^{III} is in most plentiful supply in subglacial debris, because it is the by-product of sulphide oxidation (Equation 4) and magnetite also is present in the bedrock. Fe^{3+} ions participate in sulphide oxidation (Equation 12), particularly if the weathering environment is acidic (Williamson and Rimstidt, 1994), although the acidity may be at the microscale only if the reaction is catalysed by microbes (J. Parkes, personal communication, 1999). The usual form of this reaction involves the recycling of Fe between the 2+ and 3+ oxidation states. Equation (12) shows that Fe^{3+} is reduced to Fe^{2+} and that the Fe^{2+} is converted back into Fe^{3+} in the presence of O_2 (Singer and Stumm, 1970), as shown in Equation (13), so propagating the first reaction. Equation (12) suggests that the microchemical weathering environment on the sulphide surface may be acidic and anoxic, whereas Equation (13) suggests that the bulk solution may be alkaline and oxic. Hence, the rate of the overall reaction shown in Equation (14) depends on the diffusion of Fe^{3+} and Fe^{2+} into and out of the microenvironment. Comparison of Equations (4) and (14) shows that there is a small increase in the amount of SO_4^{2-} liberated by Fe^{3+} oxidation of sulphide per unit of oxygen (*c*. 414 cf. *c*. 386 μeq/L, assuming that the water initially is saturated with O_2 at 0 °C and that there are no other subglacial sources of O_2). Hence, even this reaction cannot generate the high SO_4^{2-} concentrations found in Type A waters.

If there is no Fe^{2+} recycling step (Equation 13), as might be the case in an anoxic environment, Fe^{III} oxidation of sulphide has great potential to liberate acidity and to dissolve carbonates, as shown by Equation (15), and produces solutions with higher $HCO_3^- : SO_4^{2-}$ ratios than the reaction shown in Equation (4). Hence, suboxic oxidation of sulphides has the potential to generate higher quantities of HCO_3^-

from carbonate than oxidation of sulphides by O_2. The precise amount of $CaCO_3$ that is dissolved per unit of Fe^{3+} that is reduced, and hence the $SO_4^{2-}:HCO_3^-$ ratio, depends upon the source of the Fe^{3+} and the fate of the Fe^{2+}. For example, if the Fe^{3+} is derived from Fe^{III} oxyhydroxides and the Fe^{2+} is precipitated as Fe^{II} oxyhydroxide, then the reaction takes on the form shown by Equation (16a). Under these circumstances, the $SO_4^{2-}:HCO_3^-$ ratio is 1 : 1 in units of equivalents, rather than 1 : 4 as in Equation (15). This also is the case if Fe^{3+} is derived from silicate and the Fe^{2+} sink is Fe^{II} oxyhydroxide (Equation 16b).

This analysis demonstrates that coupled sulphide oxidation and carbonate dissolution is not restricted to oxic environments. Equations (16a) and (16b) demonstrate that SO_4^{2-} and HCO_3^- may continue to increase with a ratio of *c*. 1 : 1 under anoxic conditions. Equation (17) shows that it is possible to generate excess HCO_3^- with respect to SO_4^{2-} if suitable sources of Fe^{III} and sinks of Fe^{II} exist. Under certain conditions, $SO_4^{2-}:HCO_3^-$ ratios of 1 : 4 may be derived. We have no means of confirming this hypothesis from the data set presented here, although analysis of the $\delta^{18}O$ of SO_4^{2-} in runoff suggests that it is likely (Bottrell and Tranter, in press).

A 0·76 : 1 line, with an intercept of 220 μeq/L to allow for alkalinity generated by carbonate hydrolysis (see the regression analysis above), has been added to Figure 4b as an aid to interpretation of the data set. Points lying along this line suggest that solute has been acquired by a coupling of *c*. 4 : 1 of carbonate:silicate dissolution and sulphide oxidation, as described by Equations (4), (5), (16a) and (16b). Points lying below the line are the result of a greater proportion of the sulphide oxidation being coupled to silicate weathering (Equation 5). Type A waters with high SO_4^{2-} concentration (>700 μeq/L) lie largely above the 0·76 : 1 line. Those with significantly higher HCO_3^- concentrations relative to SO_4^{2-} lie along two main trends that possibly have a $HCO_3^-:SO_4^{2-}$ ratio of 4 : 1. The first group lies along a 4 : 1 line that intersects the 0·76 : 1 line at a SO_4^{2-} concentration of *c*. 230 μeq/L, whereas the second group (albeit three points) lies along a 4 : 1 line that intersects the 0·76 : 1 line at a SO_4^{2-} concentration of *c*. 880 μeq/L. One possible interpretation of the location of these Type A waters is as follows. High SO_4^{2-} Type A waters lying along the 0·76 : 1 line most probably are the result of oxidation of sulphide, either by oxygen derived from basal ice (i.e. Equation 4) or by sub-oxic oxidation of sulphides by Fe^{3+} derived from Fe^{III} oxyhydroxides and magnetite, using Fe^{II} oxyhydroxides as an Fe^{2+} sink (Equation 16a). When all reactive Fe^{III} oxyhydroxide is used up, reactions involving Fe^{3+} derived from silicates take over (Equation 15), giving rise to the 4 : 1 line. It seems that the Fe^{2+} produced by this reaction is used to replace the Fe^{3+}, rather than to form Fe^{II} oxyhydroxides (Equation 16a). Hence, a reaction shown hypothetically by Equation (17) is suggested.

This explanation of Type A water chemistry requires an anoxic chemical weathering environment with a high rock:water ratio in which secondary weathering products are forming, because Fe is being incorporated into exchange sites rather than oxyhydroxides. The formation of secondary weathering products, such as clays, also might explain why the Si concentration of these waters is low, as Si may be either incorporated into clay mineral lattices or adsorbed onto clay surfaces (Siever and Woodford, 1973; Lerman, 1979). The presence of two clusters of points lying along 4 : 1 lines suggests that waters of different initial oxygen saturation have accessed the Type A chemical weathering environment.

Type A waters seem to come from very isolated parts of the distributed system, but are sampled in englacially connected holes. This could be a result of the inverse water pressure relationship between these parts of the system and the main channel described by Gordon *et al*. (1998). These areas are unloaded and local porewater pressure in subglacial till falls as the pressure in the main channel rises. By contrast, load shifts to these areas of the bed as pressure in the main channel falls, porewater pressure rises and water is forced to rise from the bed into the englacial system if porewater pressure in these areas locally and transiently exceeds ice overburden.

Controls on the chemical composition of Type B waters

The majority of subglacial waters were of this type, and were collected from boreholes with basal connections (Table V). They are intermediate in composition between Types A and C (Figure 2). They

correspond to the Mode 3 waters, which are believed to be representative of waters from a distributed drainage system (Tranter *et al.*, 1997a). Concentrated Type B waters were sampled from Hole 62, which was high standing and showed relatively small fluctuations in water level or stratification (Figure 3), signifying limited exchange of subglacial waters with the surrounding drainage system, and therefore prolonged contact between water and rock flour or bedrock. By contrast, Hole 68 provided the most dilute samples, was low standing shortly after sampling commenced and exhibited significant diurnal fluctuations in water level (Figure 3), indicating better connectivity with the main channel. It could be argued, therefore, that waters sampled from the base of Hole 68 have been in transit through the distributed drainage system for shorter periods than those sampled from Hole 62, because the transmissivity of the drainage system in the vicinity of Hole 68 is likely to be higher (Hubbard *et al.*, 1995). If this is the case, at least some of the linear distribution of samples that define Type B waters in Figure 2 could arise from variations in the residence time of waters in the distributed drainage system (i.e. quasi-kinetic controls are in operation).

Table VI presents the results of simple linear regression of Ca^{2+} versus SO_4^{2-} and HCO_3^- for all borehole water types. There are no statistically significant differences between the regression slopes for Ca^{2+} or $(Ca^{2+} + Mg^{2+})$ versus SO_4^{2-} for Type A and B waters. This suggests that the linkage between sulphide oxidation and carbonate–silicate dissolution is essentially similar in the chemical weathering environments that generate these water types. The regression slope of HCO_3^- versus SO_4^{2-} is less than 1 (Table VI), implying that some of the protons derived from sulphide oxidation are used to weather silicates (Equation 5). Most SO_4^{2-} concentrations are <414 μeq/L, the limit of SO_4^{2-} generated from the oxidation of sulphides by water initially saturated with O_2 at the altitude of the glacier terminus. This may suggest that the O_2 concentration of input waters is the limiting factor on the extent of sulphide oxidation, but caution is necessary with this interpretation because the O_2 content of supraglacial ice- and snow-melt both decrease with altitude, and the O_2 saturation is seldom 100% (Brown *et al.*, 1994b). What is clear is that SO_4^{2-} concentrations >414 μeq/L suggest that elements of the distributed drainage system that generate Type B waters are likely to be anoxic, and participate in Fe^{3+} oxidation of sulphide, such as shown by Equations (16a) and (16b). The spatial extent of the inferred anoxia clearly will increase as the O_2 content of the input waters decreases. Some of the waters with SO_4^{2-} concentrations of *c.* 500 μeq/L appear to be similar to Type A waters in that they depart from the 0·76 : 1 line along a 4 : 1 line. Hence, it is possible that reactions similar to Equation (17) occur in the more hydrologically isolated parts of the distributed system that give rise to Type B waters, and hence that there may be a spectrum of Type B through Type A chemical weathering environments in the distributed drainage system.

The better basal connectivity of the boreholes containing Type B waters suggests that the chemical weathering environment is hydrologically more efficient than those giving rise to Type A waters. Residence time and the formation of secondary silicates probably are the key discriminating variables in producing the different Si concentrations relative to the major ions. The more efficient parts of the distributed drainage system that give rise to Type B waters have lower residence times and lower rock:water ratios, and so have less potential to form secondary silicates.

We believe that Type B waters are produced in the distributed system, yet they are sampled in the variable pressure axis (VPA), the zone in which boreholes record diurnal flucuations in basal water pressures (Hubbard *et al.*, 1995). This suggests that they are in the process of draining from the distributed system to the channel. They are not usually found in unconnected holes (Table V) because these are overpressured relative to the distributed system by supraglacial water and/or drilling fluid, which keeps them from rising into the holes. It is likely that the VPA and the channel margin zones discussed in the next section are not synonymous, and that elements of the VPA away from the channel do not receive a large influx of channel-derived waters (i.e. the movement of water from the main channel may be restricted to only the most proximal part of the VPA). Porewater pressures in the more distal parts of the VPA still fluctuate as a result of forcing from the channel.

Controls on the chemical composition of Type C waters

Type C waters are the most dilute (Figure 2 and Table IV). They were sampled mainly from unconnected boreholes or from holes with basal connections (Table V). All samples were very turbid. The chemical composition is characterized by low $SO_4^{2-}:HCO_3^-$ ratios and high pH (Table IV). Type C waters contain relatively high concentrations of Si (Figure 2) and are similar to the Mode 2A waters described by Tranter *et al*. (1997a), and are believed to reside in the channel marginal zone where rock flour is depleted of reactive sulphides.

A more general criterion for the chemical evolution of Type C waters could be that reactive sulphides are in short supply along the water flow path, and that the high pH arising from carbonate hydrolysis promotes elevated rates of Si dissolution. Hence, it is possible that Type C waters could develop outside the channel marginal zone. Carbonate hydrolysis is likely to be the first reaction that these waters undergo, and is consistent with the simple regression analysis presented in Table VI. Table IV shows that Type C waters contain $(Ca^{2+} + Mg^{2+})$ and HCO_3^- concentrations that are approximately equal to that arising from carbonate hydrolysis (*c*. 250 μeq/L), and that they have relatively high pH ($8{\cdot}1 \pm 0{\cdot}8$). Higher pH promotes elevated rates of Si dissolution from silicates (Knauss and Wolery, 1986; Brady and Walther, 1989; Gratz and Bird, 1993), and, in the absence of significant sulphide oxidation, Type C waters remain at high pH for longer periods and so become enriched in Si relative to Ca^{2+}, HCO_3^- and SO_4^{2-}. Concentrations of Ca^{2+} and HCO_3^- remain relatively low because there are only minor reactive sulphide sources with which to dissolve carbonates and silicates. Elevated Si concentrations also can be generated in the channel marginal zone if waters become entrapped in the zone during flooding. Then, the only reaction that is likely to occur in the absence of sulphide oxidation is silica dissolution.

Table VI shows that the slope of the best-fit linear regression equation of $(Ca^{2+} + Mg^{2+})$ versus SO_4^{2-} is *c*. 2, suggesting that the limited sulphide oxidation that occurs in the chemical weathering environments dissolves principally carbonates (Equation 4). The slope of the best-fit regression equation of HCO_3^- versus SO_4^{2-} should be *c*. 1, and the derived value of $1{\cdot}53 \pm 0{\cdot}47$ is consistent with this interpretation (Table VI). The high Na^+ and K^+ concentrations of Type C waters (Figure 4d) probably arise from silicate dissolution and surface exchange of these monovalent ions for the divalent ions liberated by carbonate dissolution. High rock:water ratios favour the adsorption of divalent ions with respect to monovalent ions (Stumm and Morgan, 1996).

Finally, the elevated $HCO_3^-:SO_4^{2-}$ ratios of these waters may indicate that there is a HCO_3^- source in the channel marginal zone. Microbes are known to populate areas of high rock:water ratios (Sharp *et al*., 1999), such as the channel marginal zone, and this zone also may receive in-washed organic carbon and nutrient from the glacier surface during rising discharge. Hence, it is possible that limited microbial oxidation of organic carbon occurs, so generating a source of CO_2 that allows some carbonation of silicates and carbonates.

The association between the chemical compositions of subglacial waters and bulk runoff

It is important to consider whether or not the three water types delimited above are consistent with the chemical characteristics of bulk runoff, because if this is the case, the chemical weathering reactions described above can be assumed to occur not only in the small area of the bed that we sampled but in other hydrologically active areas of the bed.

Scatter plots of Ca^{2+} and HCO_3^- versus SO_4^{2-} suggest that bulk runoff can be derived by diluting concentrated subglacial waters with icemelt (Figure 6a). However, scatter plots of these ions versus Si (Figure 6b) show that simple dilution alone cannot account for the composition of the bulk runoff, which is intermediate between Type B (the most frequently sampled type of subglacial water) and Type C waters. The composition of the bulk runoff is bounded by the compositions of Type B and C waters (we can safely ignore the potential impact of Type A waters on runoff because they originate from an inefficient part of the distributed drainage system and are unlikely to make a quantitatively significant contribution to runoff hydrochemistry). Variations in the concentration of the bulk runoff are consistent with dilution of a concentrated end-member

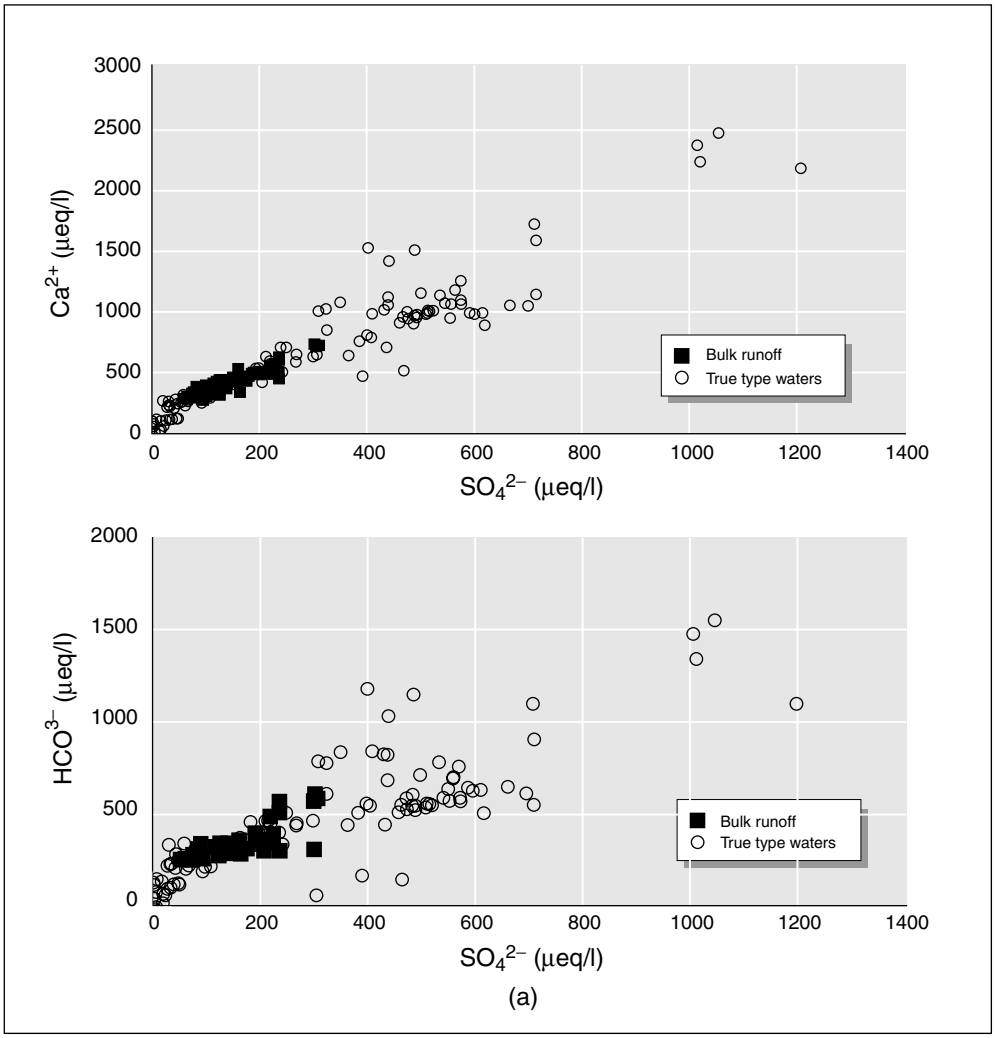

Figure 6a. Scatterplots of (a) Ca^{2+} and HCO_3^- versus SO_4^{2-}

mixture of Type B and C waters by supraglacial inputs. Hence, bulk runoff appears to be derived from a mixture of waters that have flowed through a distributed drainage system (Type B waters), through the channel marginal zone (Type C waters) and dilute supraglacial inputs. This explanation of bulk meltwater chemistry suggests that little post-mixing carbonation occurs (cf. Brown *et al*., 1994a), and hence that little atmospheric CO_2 is consumed during subglacial chemical weathering.

Bulk runoff is most dilute at high discharge, when suspended sediment concentrations also are high (Gurnell *et al*., 1994). Figure 6b suggests that dilute bulk runoff can be approximated by simple dilution of Type B waters. Hence, the impact of post-mixing reactions in the channelized drainage system apparently is small (cf. Brown *et al*., 1994a). Bulk runoff becomes more concentrated as discharge decreases. The more concentrated runoff in Figure 6b seems to require that Type B and Type C waters mix. In other words, it appears that at lower discharge, there is return flow of waters from the channel marginal zone into the channelized drainage system, and this leads to the waters having proportionally less Ca^{2+}, SO_4^{2-} and HCO_3^- with respect to Si than would arise if there was simple dilution of Type B waters. Hence, a small proportion of the dilute supraglacial

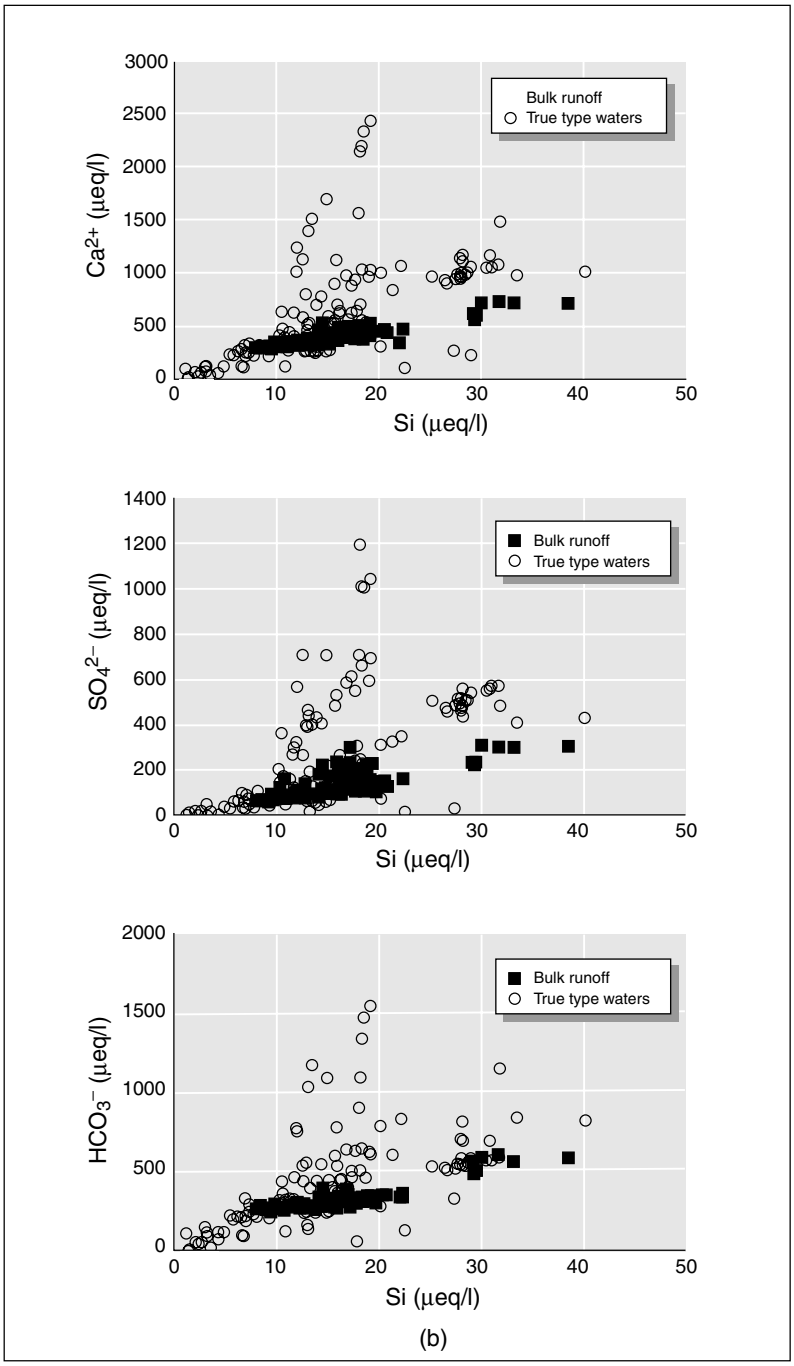

Figure 6b. Ca^{2+}, SO_4^{2-} and HCO_3^- versus Si for all true Type A, B and C borehole waters and bulk runoff

icemelt entering the channelized subglacial drainage system appears to have been held in temporary storage in channel marginal zones, and may drain from the glacier either overnight when surface melting is limited or during longer periods of recession flow.

CONCLUSIONS

The study of borehole water chemistry offers insight into subglacial hydrochemical processes that cannot be derived easily from an analysis of bulk runoff. Samples of subglacial waters collected over two melt seasons from boreholes drilled to the bed of Haut Glacier d'Arolla have a variable composition. Three types of subglacial meltwater are defined on the basis of the ratios of the major ions with respect to Si. It is possible that other types of subglacial water composition might exist, because only a limited number of boreholes from a small area of the bed were sampled, but the similarity in the composition of these waters with that of concurrent bulk runoff suggests that two of the dominant subglacial water types have been identified. The composition of the different water types conveys important information regarding the nature of the chemical weathering environment at the bed.

The principal chemical weathering mechanisms by which subglacial meltwaters in distributed drainage systems obtain solute are (i) carbonate and silicate hydrolysis, with exchange of divalent cations from solution for monovalent cations on surface exchange sites; and (ii) carbonate and silicate dissolution coupled to sulphide oxidation. The crude ratio of carbonate to silicate weathering following carbonate hydrolysis is *c*. 4 : 1. Sulphides are oxidized initially by oxygen, but may be oxidized by Fe^{3+} in anoxic environments following depletion of dissolved O_2. Dissolution of Si from silicates is likely to be promoted by the high pH that arises from hydrolysis.

Type A waters are relatively rare and exhibit high concentrations of Ca^{2+}, HCO_3^- and SO_4^{2-} relative to Si. A subglacial supply of oxidizing agent(s), additional to that provided by O_2-bearing supraglacial input, is necessary to promote the high SO_4^{2-} concentrations found. It is probable that the sulphides are oxidized by Fe^{3+} in anoxic environments. The high rock:water ratios and long residence times of waters in this weathering environment may promote the formation of secondary reaction products, such as clays, which deplete the meltwaters of Si. They might also promote the exchange of Fe^{3+} for Fe^{2+} and Ca^{2+} on silicates, so driving up the $HCO_3^- : SO_4^{2-}$ ratio.

Type B waters, the most frequently sampled, probably form in a distributed drainage system. Their composition is intermediate between Types A and C. The initial reactions to occur are carbonate and silicate hydrolysis, followed by coupled oxidation of sulphides and dissolution of carbonates and silicates. There is evidence that there are residence time or kinetic influences on the composition of these waters, with higher concentrations of ions being associated with waters in slower transit through sediments of lower hydraulic conductivity. Oxygen is depleted along the flow path, so that, on occasion, elements of the distributed drainage system may become anoxic. Type A waters therefore can be thought of as extreme examples of Type B waters, modified by the effects of formation of secondary weathering products.

Type C waters appear to be formed in channel marginal zones in the area of the bed sampled, where there are variations in discharge on a variety of time-scales, resulting in oscillating water flow into and out of the zone. This promotes the depletion of reactive sulphides and enhances the impact of carbonate hydrolysis. The lower concentrations of the major ions and higher Si concentrations in Type C waters suggest a weathering environment in which the bedrock is depleted of reactive sulphides. Hence, following hydrolysis, solute is supplied via the slow dissolution of carbonates, silicates and Si, fuelled by limited amounts of sulphide oxidation and by microbial oxidation of organic matter. The high pH of these waters favours relatively high rates of Si dissolution, and therefore relatively high Si concentrations. The formation of secondary weathering products, such as clays, is likely to be hindered by the relatively short residence time of water in these environments.

A comparison of the chemical composition of the bulk runoff and the subglacial waters shows that the bulk runoff is most similar to Type B and C waters. Dilute bulk runoff approximates the composition of diluted Type B water, whereas more concentrated bulk runoff approximates a mixture of Type B and C waters. These features suggest that supraglacial input to the bed is stored temporarily in the channel marginal zone during rising discharge and that waters from the distributed system enter channels increasingly at their heads. By

contrast, waters from the channel margins return to the channel at low discharge and mix with distributed system waters at times when dilution by surface inputs is minimal.

The above model is radically different from the two-component mixing models of the earlier literature in terms of the primary water flow paths and the variability in the chemical composition of the concentrated components (Collins, 1979; Lecce, 1993; cf. Sharp *et al.*, 1995b). It is very different from the one-reservoir model propounded by Collins (1996). This analysis suggests that subglacial chemical weathering schemes inferred from bulk runoff hydrochemistry may be erroneous (e.g. Tranter *et al.*, 1993). We suggest that similar types of chemical reactions can occur to greater or lesser extents across the spectrum of subglacial environments, and that the oxidizing agent used to degrade sulphides also must vary. Microbial influences on subglacial chemical weathering, which may drive large sections of the bed into anoxia, now need urgent consideration, as does the role (and source) of Fe^{III} in the oxidation of sulphides if the chemical weathering schemes derived from small temperate valley glaciers are to be scaled-up to large polythermal ice masses.

We conclude that subglacial chemical weathering is distinctive from most other types of geochemical weathering in earth surface environments, which are driven mainly by atmospheric CO_2 or biologically derived CO_2 in soils (Drever, 1988; Berner and Berner, 1996). Subglacial chemical weathering is dependant on sulphide oxidation and Fe^{III} reduction, and differs from the chemical weathering undertaken by acid mine drainage waters in that the bulk pH usually is 7–9, because of the presence of comminuted bedrock. This limits the amount of aluminosilicate dissolution that can occur (Lerman, 1979).

Carbonates are preferentially chemically weathered with respect to silicates. Hence, the solute found in glacial runoff is derived largely from bedrock, and solute derived from the atmosphere, including CO_2, is minimal. The O_2, rather than the CO_2, content of waters input to the subglacial drainage system is a major determinant on the chemical weathering potential of the meltwaters.

ACKNOWLEDGEMENTS

This research was funded by NERC via a studentship to HRL (GT4/93/113) and Grants Nos. GR3/8114, GR9/1018, GR9/1126 and GR9/2550. Counting Crows, Anna Begins on *Across the Wires*, provided the inspiration to get this brick buried.

REFERENCES

Berner EK, Berner RA. 1996. *Global Environment: Water, Air and Geochemical Cycles*. Prentice Hall: Englewood Cliffs, NJ.

Blake EW, Clarke GKC. 1991. Subglacial water and sediment samplers. *Journal of Glaciology* **37**: 188–190.

Bottrell SH, Tranter M. In press. Sulphide oxidation under partially anoxic conditions at the bed of Haut Glacier d'Arolla, Switzerland. *Hydrological Processes*.

Brady PV, Walther JV. 1989. Controls on silicate dissolution rates in neutral and basic pH solutions at 25 °C. *Geochimica et Cosmochimica Acta* **53**: 2823–2830.

Brown GH, Sharp MJ, Tranter M, Gurnell AM, Nienow PW 1994a. The impact of post–mixing chemical reactions on the major ion chemistry of bulk meltwaters draining the Haut Glacier d'Arolla, Valais, Switzerland. *Hydrological Processes* **8**: 465–480.

Brown GH, Tranter M, Sharp MJ, Davies TD, Tsiouris S. 1994b. Dissolved oxygen variations in Alpine glacial meltwaters. *Earth Surface Processes and Landforms* **19**: 247–253.

Coachman LK, Hemmingson E, Scholader PF. 1958. Gases in glaciers. *Science* **127**: 1288–1289.

Collins DN. 1978. Hydrology of an alpine glacier as indicated by the chemical composition of meltwater. *Zeitschrift fur Gletscherkunde und Glazialgeologie* **13**: 219–238.

Collins DN. 1979. Quantitative determination of the subglacial hydrology of two alpine glaciers. *Journal of Glaciology* **23**: 347–363.

Collins DN. 1996. Dissolution kinetics, transit times through subglacial hydrological pathways and diurnal variations of solute content of meltwaters draining from an Alpine glacier. *Hydrological Processes* **9**: 897–910.

Drever JI. 1988. *The Geochemistry of Natural Waters*, 2nd edn. Prentice Hall: Englewood Cliffs, NJ.

Fairchild IJ, Bradby L, Sharp M, Tison J-L. 1994. Hydrochemistry of carbonate terrains in alpine glacial settings. *Earth Surface Processes and Landforms* **19**: 33–54.

Fountain AG. 1992. Subglacial flow inferred from stream measurements at South Cascade Glacier, Washington, U.S.A.. *Journal of Glaciology* **38**: 51–64.

Fountain AG. 1994. Borehole water level variations and implications for the subglacial hydraulics of South Cascade Glacier, Washington, USA. *Journal of Glaciology* **40**: 293–304.

Fountain AG, Walder JS. 1998. Water flow through temperate glaciers. *Reviews of Geophysics* **36**: 299–328.
Garrels RM, Howard P. 1957. Reactions of feldspar and mica with water at low temperatures and pressure. *Clays Clay Minerals* **6**: 68–88.
Garrels RM, Christ CL. 1965. *Solutions, Minerals and Equilibria*. Freeman Cooper: San Francisco.
Gordon S, Sharp M, Hubbard B, Smart C, Ketterling B, Willis I. 1998. Seasonal organization of subglacial drainage inferred from measurements in boreholes. *Hydrological Processes* **12**: 105–134.
Gratz AJ, Bird P. 1993. Quartz dissolution: negative crystal experiments and a rate law. *Geochimica et Cosmochimica Acta* **57**: 965–976.
Gurnell AM. 1987. Suspended sediment. In *Glacio- fluvial Sediment Transfer: an Alpine Perspective*, Gurnell AM, Clark MJ (eds). Wiley: Chichester; 305–354.
Gurnell AM, Brown GH, Tranter M. 1994. A sampling strategy to describe the temporal characteristics of an Alpine proglacial stream. *Hydrological Processes* **8**: 1–25.
Hallet B. 1976. Deposits formed by the subglacial precipitation of $CaCO_3$. *Geological Society of America Bulletin* **87**: 1003–1015.
Harbor JM, Sharp M, Copland L, Hubbard B, Nienow P, Mair D. 1997. Influence of subglacial drainage conditions on the distribution of velocity in a glacier cross section. *Geology* **25**: 739–742.
Holland HD. 1978. *The Chemistry of the Atmosphere and Oceans*. Wiley: New York.
Hubbard BP, Sharp MJ, Willis IC, Nielsen MK, Smart CC. 1995. Borehole water–level variations and the structure of the subglacial hydrological system of the Haut Glacier d'Arolla, Valais Switzerland. *Journal of Glaciology* **41**: 140–148.
Kamb B. 1986. Glacier surge mechanism based on linked cavity configuration of the basal water conduit system. *Journal of Geophysical Research* **92**(B9): 9083–9100.
Knaus KG, Wolery TJ. 1986. Dependence of albite dissolution kinetics on pH and time at 25 °C and 70 °C. *Geochimica et Cosmochimica Acta* **50**: 2481–2497.
Lamb HR, Tranter M, Brown GH, Hubbard BP, Sharp MJ, Smart CC, Willis IC, Nielsen MK. 1995. The composition of subglacial meltwaters sampler from boreholes at the Haut Glacier d'Arolla, Switzerland. *International Association of Hydrological Sciences Publication* **228**: 395–403.
Lecce SA. 1993. Flow separation and diurnal variability in the hydrology of Coness Glacier, Sierra Nevada, California, U.S.A. *Journal of Glaciology* **32**: 407–421.
Lerman A. 1979. *Geochemical Processes: Water and Sediment Environments*. Wiley: New York.
Moses CO, Herman JS. 1991. Pyrite oxidation at circumneutral pH. *Geochimica et Cosmochimica Acta* **55**: 471–482.
Nicholson RV, Gillham RW, Reardon EJ. 1988. Pyrite oxidation in carbonate-buffered solution: 1. Experimental kinetics. *Geochimica et Cosmochimica Acta* **52**: 1077–1085.
Nienow PW, Sharp MJ, Willis IC. 1998. Seasonal changes in the morphology of the subglacial drainage system, Haut Glacier d'Arolla, Switzerland. *Earth Surface Processes and Landforms* **23**: 825–843.
Petrovic R. 1981. Kinetics of dissolution of mechanically comminuted rock-forming oxides and silicates—II. Deformation and dissolution of oxides and silicates in the laboratory and at the Earth's surface. *Geochmica et Cosmochimica Acta* **45**: 1675–1686.
Plummer LN, Wigley TML. 1976. The dissolution of calcite in CO_2-saturated solutions at 25 °C and 1 atmosphere total pressure. *Geochimica et Cosmochimica Acta* **40**: 191–202.
Raiswell R. 1984. Chemical models of solute acquisition in glacial melt waters. *Journal of Glaciology* **30**: 49–57.
Richards KS, Sharp M, Arnold N, Gurnell A, Clark M, Tranter M, Nienow P, Brown G, Willis I, Lawson W. 1996. An integrated approach to studies of glacier hydrology and water quality: field and modelling studies at the Haut Glacier d'Arolla, Switzerland. *Hydrological Processes* **10**: 479–508.
Sharp MJ. 1991. Hydrological inferences from meltwater quality data—the unfulfilled potential. *Proceedings of the British Hydrological Society National Symposium, Southampton, 16–18 September*: 5.1–5.8.
Sharp MJ, Willis IC, Arnold N, Nienow P, Lawson W, Tison J-L. 1993. Geometry, bed topography and drainage system structure of the Haut Glacier d'Arolla, Switzerland. *Earth Surface Processes and Landforms* **18**: 557–561.
Sharp M, Brown GH, Tranter M, Willis IC, Hubbard BP. 1995a. Some comments on the use of chemically-based mixing models in glacier hydrology. *Journal of Glaciology* **41**: 241–246.
Sharp M, Tranter M, Brown GH, Skidmore M. 1995b. Rates of chemical denudation and CO_2 drawdown in a glacier-covered alpine catchment. *Geology* **23**: 61–64.
Sharp M, Parkes J, Cragg B, Fairchild IJ, Lamb H, Tranter M. 1999. Widespread bacterial populations at glacier beds and their relationship to rock weathering and carbon cycling. *Geology* **27**(2): 107–110.
Siever R, Woodford N. 1973. Sorption of silica by clay minerals. *Geochimica et Cosmochimica Acta* **37**: 1851–1880.
Singer PC, Stumm W. 1970. Acid mine drainage: the rate limiting step. *Science* **167**: 1121–1123.
Smart CC. 1996. Statistical evaluation of glacier boreholes as indicators of basal drainage systems. *Hydrological Processes* **10**: 599–614.
Souchez RA, Lemmens MM. 1987. Solutes. In *Glacio-fluvial Sediment Transfer*, Gurnell AM, Clark MJ (eds). Wiley: Chichester; 285–303.
Stone DB, Clarke GKC. 1996. *In situ* measurements of basal-water quality and pressure as an indicator of the character of subglacial drainage systems. *Hydrological Processes* **10**: 615–628.
Stumm W, Morgan JJ. 1996. *Aquatic Chemistry: Chemical Equilibria and Rates in Natural Waters*. Wiley: Chichester.
Tranter M, Raiswell R. 1991. The composition of the englacial and subglacial components in bulk meltwaters draining the Gornergletscher. *Journal of Glaciology* **37**: 59–66.
Tranter M, Brown GH, Raiswell R, Sharp MJ, Gurnell AM. 1993. A conceptual model of solute acquisition by Alpine glacial meltwaters. *Journal of Glaciology* **39**: 573–581.
Tranter M, Brown GH, Hodson A, Gurnell AM, Sharp MJ. 1994. Variations in nitrate concentration of glacial runoff in Alpine and sub-Polar environments. *International Association of Hydrological Sciences Publication* **223**: 299–311.
Tranter M, Sharp MJ, Brown GH, Willis IC, Hubbard GH, Nielsen MK, Smart CC, Gordon S, Tulley M, Lamb HR. 1997a. Variability in the chemical composition of *in situ* subglacial meltwaters. *Hydrological Processes* **11**: 59–77.

Tranter M, Lamb HR, Bottrell SH, Raiswell R, Sharp MJ, Brown GH. 1997b. Preliminary investigation into the utility of $\delta^{34}S$ and $^{87}Sr/^{86}Sr$ as tracers of bedrock weathering and hydrologic flowpaths beneath an Alpine glacier. *International Association of Hydrological Sciences Publication* **244**: 317–324.

Waddington BS, Clarke GKC. 1995. Hydraulic properties of subglacial sediment determined from the mechanical response of waterfilled boreholes. *Journal of Glaciology* **41**: 112–124.

Wadham JL, Hodson AJ, Tranter M, Dowdeswell JA. 1998. The hydrochemistry of meltwaters draining a polythermal-based, high Arctic glacier, south Svalbard: I. The ablation season. *Hydrological Processes* **12**: 1825–1849.

Walser JS, Fowler A. 1994. Channelised subglacial drainage over a deformable bed. *Journal of Glaciology* **40**: 439–445.

Weertman J. 1972. General theory of water flow at the base of a glacier or ice sheet. *Reviews in Geophysics and Space Physics* **10**: 287–333.

Williamson MA, Rimstidt JD. 1994. The kinetics and electrochemical rate-determining step of aqueous pyrite oxidation. *Geochimica et Cosmochimica Acta* **58**: 5443–5454.

